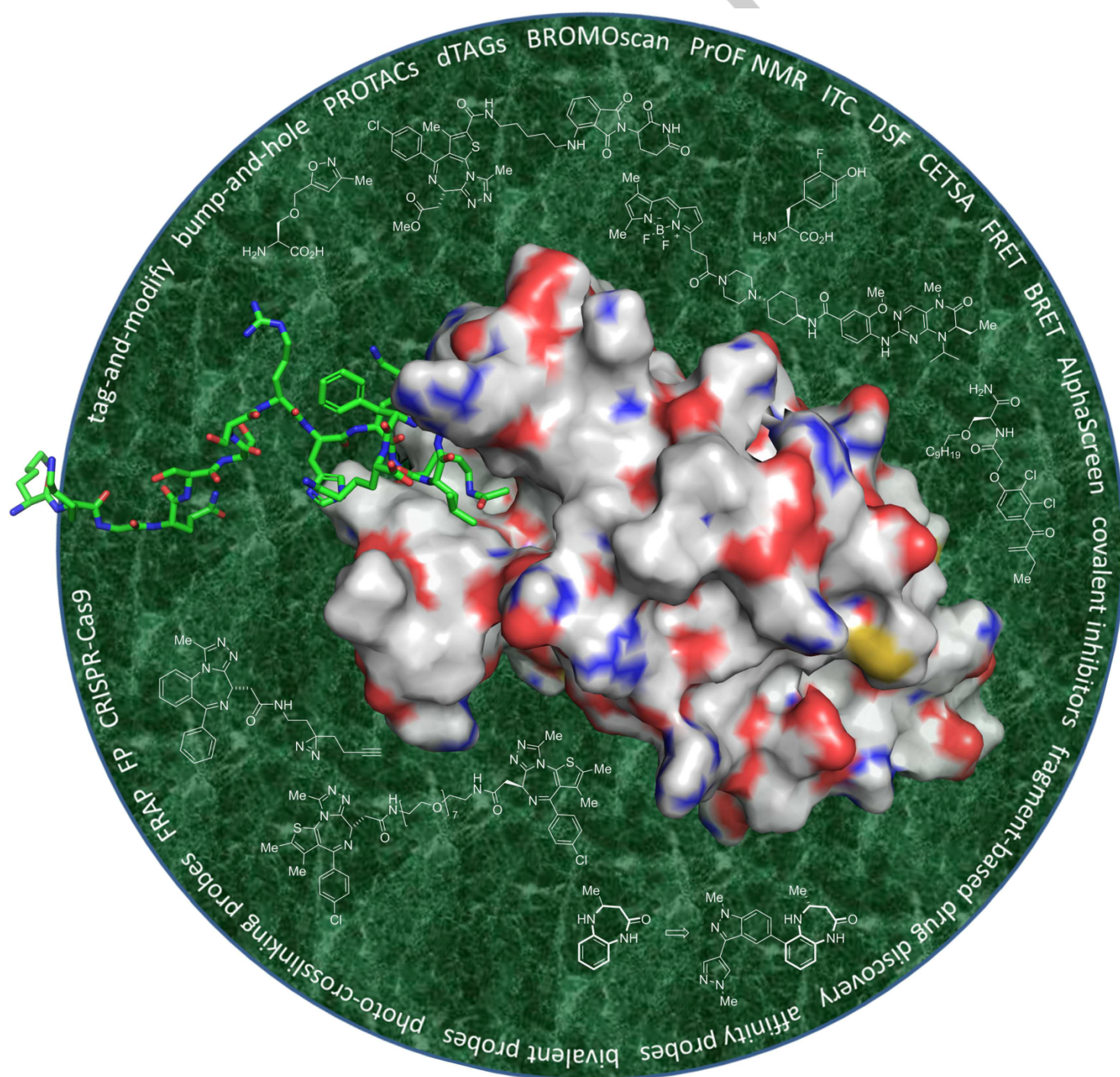


Chemical epigenetics: the impact of chemical- and chemical biology techniques on bromodomain target validation

Matthias Schiedel, Mustafa Moroglu, David M. H. Ascough, Anna E. R. Chamberlain, Jos J. A. G. Kamps, Angelina R. Sekirnik, and Stuart J. Conway^{*[a]}



Abstract: Epigenetics is currently the focus of intense research interest across a broad range of disciplines due to its importance in a multitude of biological processes and disease states. At the molecular level, epigenetic functions result partly from modification of the nucleobases in DNA and RNA, and/or post-translational modifications (PTMs) of histone proteins. Much evidence has emerged to demonstrate that these modifications are dynamic, with cellular machinery identified to modulate and interpret the marks. Our focus is on bromodomains, which bind to acetylated lysine (KAc) residues. Progress in the study of bromodomains, and the development of bromodomain ligands, has been rapid. These advances have been underpinned by many disciplines, but chemistry and chemical biology techniques have undoubtedly played a very significant role. Here we review the key chemistry and chemical biology approaches that have furthered our study of bromodomains, enabled the development of bromodomain ligands, and played a critical role in the validation of bromodomains as therapeutic targets.

1. Introduction

1.1. Article aim and scope

Target validation is widely recognized as the foundation of a successful drug-discovery programme. If the programme is built upon a solid, well-validated, target and hypothesis it stands the best chance of being successful and delivering a compound that shows the desired biological, and ultimately clinical, effects. However, if the programme does not have a solid foundation, then it will not be successful. Many disciplines are necessary for effective target validation. Received wisdom has been that 'medicinal chemistry' is mainly in the purview of industrial scientists, whereas 'chemical biology' is more typically viewed as an academic pursuit. Yet target validation is at the nexus of these two areas, and both medicinal chemistry and chemical biology have essential roles to play in this process. Not surprisingly then, both academic and industrial scientists, and importantly academic-industrial partnerships, have contributed towards target validation studies. Here we focus on bromodomain ligand discovery, which has been an area of intense interest over the last decade, with a number of bromodomain ligands in clinical trials. Much of the target validation work in this area has been pre-competitive, with notable successes in both validating and

invalidating hypotheses. Key contributions have come from both academia and industry, and a variety of chemical- and chemical biology-based techniques have played important roles in this work.

1.2. Introduction to epigenetics and bromodomains

The term 'epigenetics' has evolved since its first use by Waddington;^[1] and a phenomenon is now defined as epigenetic if it encompasses a "stably heritable phenotype resulting from changes in chromosome without alterations in DNA sequence".^[2] Key molecular mechanisms that underpin epigenetic phenomena include the addition of methyl groups, and other marks, to DNA,^[3] modification of the nucleobases in RNA,^[4] and the post-translational modification (PTM) of histone proteins.^[5] A multitude of studies have demonstrated that these modifications are dynamic, with cellular machinery identified to modulate and interpret these marks. The quantity and complexity of the PTMs found on histones led to the idea of a histone code,^[6] and this code analogy has been extended to describe enzymes that add epigenetic marks as writers, and enzymes that remove them as erasers. A third class of proteins has been identified that bind to the marks, mediating protein-chromatin or protein-protein interactions (PPIs) to facilitate the assembly of large transcription complexes. These proteins are viewed as interpreting the histone code and are termed readers.^[5c]

Of the reader proteins studied to date, the bromodomains, which bind to acetylated lysine (KAc), have been the focus of much attention.^[7] There are 61 bromodomains in the human proteome, found in 46 different proteins. These include proteins which function as histone methyltransferases (e.g. ASH1L/KMT2H),^[8] histone acetyl transferases and HAT-associated proteins [e.g. the general control of amino acid synthesis protein 5-like 2 (GCN5L2/KAT2A), P300/CBP-associated factor (PCAF/KAT2B)],^[7b, 9] ATP-dependent chromatin remodeling complexes [e.g. bromodomain adjacent to zinc finger domain protein 1B (BAZ1B)],^[10] transcriptional co-activators [e.g. tripartite motif-containing proteins (TRIMs)],^[11] nuclear-scaffolding proteins [e.g. polybromo 1 (PBRM1/PB1)],^[12] helicases [e.g. SWI/SNF-related matrix-associated actin-dependent regulators of chromatin subfamily A (SMARCA)],^[13] and the BET family of bromodomain-containing proteins.^[14] Despite having significant sequence variations, bromodomains feature a conserved overall fold that comprises a left-handed bundle of four α -helices (named α_Z , α_A , α_B and α_C) linked by two loop regions of variable length (the ZA and BC loops). Bromodomains are grouped into eight sub-families (I-VIII) based on their structural and sequence homology.^[15] The majority of bromodomains bind their cognate proteins (or KAc-mimicking small molecule ligands) through interaction with a highly conserved asparagine (Asn) residue. The KAc-binding pocket is predominantly hydrophobic, but a structurally-conserved network of water molecules forms its floor (Figure 1). Analysis of phylogenetically diverse bromodomain X-ray crystal structures reveals that this water network is conserved.^[16] Computational studies indicate that exchange of these water molecules is possible without a ligand bound,^[17] but these water molecules are present in most ligand-bound bromodomain X-ray crystal structures.^[18] Exceptions to this are

[a] Dr. M. Schiedel, M. Moroglu, D. M. H. Ascough, A. E. R. Chamberlain, J. J. A. G. Kamps, Dr. A. R. Sekirnik, Prof. Dr. S. J. Conway
Department of Chemistry,
Chemistry Research Laboratory,
University of Oxford,
Mansfield Road, Oxford OX1 3TA, United Kingdom

REVIEW

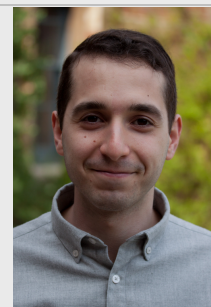
the BRG/PB1, SMARCA2 and SMARCA4 bromodomains, where this water network can be displaced, providing selectivity over other bromodomains, including the BET family, in which the water molecules cannot be displaced.^[19] Application of computational tools allows assessment of the stability of the water molecules found in the KAc-binding pocket and ZA channel of bromodomains, which is essential for structure-based ligand design.^[20] Further details of the structural features and biological functions of bromodomains have been extensively reviewed elsewhere.^[15, 21]

Phenotypic screening identified the bromodomain and extra terminal domain (BET) family of bromodomain-containing proteins as a potential therapeutic target in a number of oncology indications.^[22] The defined, largely lipophilic, KAc-binding pocket that is characteristic of many human bromodomains has allowed the development of drug-like small molecule ligands for a range of bromodomains.^[16, 21a, 23] Eleven BET bromodomain ligands are being, or have been, investigated in ~20 clinical trials for a range of indications.^[24] Progress has also been made in the development of ligands for non-BET bromodomains. These advances have been underpinned by many disciplines, but chemistry and chemical biology techniques have undoubtedly played a very significant role. Our focus here is on the technology that has underpinned this work, and not the ligands themselves, as the progress in bromodomain ligand development has been reviewed extensively elsewhere.^[5a, 16, 21a, 23, 25] This article considers the biochemical techniques and assays, the use of unnatural amino acids, fragment-based approaches, and the development of functional probes, which have been applied to the study of bromodomains. We apologize to authors whose work is not included as a result of the specific emphasis of this review.

Matthias Schiedel is postdoctoral DFG fellow working at the Chemistry Research Laboratory in Oxford. He studied Pharmacy at the University of Freiburg. At the same university, he received his PhD for the development of sirtuin inhibitors. His current research focuses on the development of bromodomain ligands.



Mustafa Moroglu obtained his MSci from Queen Mary, University of London. Mustafa is currently a DPhil student in Synthesis for Biology and Medicine – Centre for Doctoral Training at Keble College, University of Oxford, under the supervision of Prof. Stuart J. Conway.



David Ascough graduated with an MChem from the University of Oxford. David is currently pursuing a DPhil in Synthesis for Biology and Medicine – Centre for Doctoral Training at Wadham College, University of Oxford.



Anna Chamberlain graduated with an MSci in Chemistry from the University of Bristol. She is currently a doctoral candidate in the Synthesis for Biology and Medicine Centre for Doctoral Training (SBM-CDT, Oxford) with interests in development of methodology, synthesis and drug discovery.



Jos Kamps obtained his MSc in Organic Chemistry at the Radboud University Nijmegen. He is currently a doctoral candidate in the synthesis for biology and medicine center for doctoral training (SBM-CDT, Oxford), working under the supervision of Prof. Timothy D. W. Claridge and Prof. Christopher J. Schofield.



Angelina Sekirnik obtained an MChem from the University of Oxford. Under the supervision of Prof. Stuart J. Conway, she was awarded a DPhil in Systems Approaches to Biomedical Sciences in 2016, and was a recipient of an EPSRC Doctoral Prize.



Stuart Conway was raised in West Sussex in the UK, and obtained a BSc in Chemistry with Medicinal Chemistry at the University of Warwick, followed by a PhD from the University of Bristol studying with Prof. David Jane and Prof. Jeff Watkins FRS. After a post-doctoral position at the University of Cambridge with Prof. Andrew Holmes FRS, he was appointed to a Lectureship in Bioorganic at the University of St Andrews. He moved to the University of Oxford in 2008 where he is a Professor of Organic Chemistry. His research focuses on the use of organic chemistry to solve biological questions, with a particular interest in epigenetics.

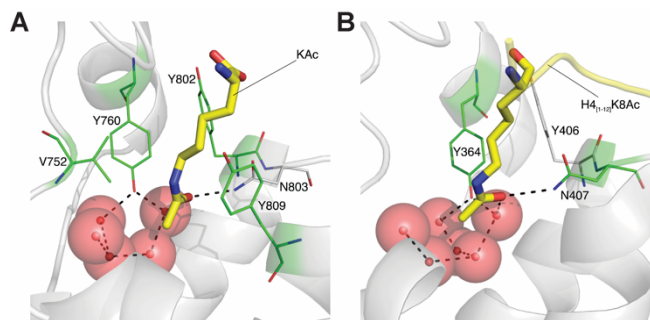


Figure 1. A) The X-ray crystal structure of KAc (carbon = yellow) bound to the PCAF bromodomain (PDB ID: 5FE0). The residues mutated by Zhou and co-workers are highlighted in green. B) The X-ray crystal structure of the histone mimicking peptide H4_[1-12]K8Ac (carbon = yellow) bound to the bromodomain of Gcn5p (PDB ID: 1E6I). Residues mutated by Owen *et al.* are highlighted in green.

2. Biochemical techniques applied to the study of bromodomains

In this section we consider the use of mutagenesis and CRISPR Cas-9 in the study of bromodomains. These techniques allow the key residues involved in ligand binding to be probed in a complementary manner to SAR studies using small molecules. CRISPR allows protein modulation or complete removal in cells. The development of *in vitro* and in cell assays is also discussed. These assays are essential to enable rapid development and validation of bromodomain ligands.

2.1. Mutagenesis studies to investigate the histone-binding ability of bromodomains

Site-directed mutagenesis can be used to probe the role of an individual residue or multiple amino acids in a protein-ligand interaction. Typically, this is accomplished by replacement of the residues that form intermolecular interactions with an amino acid that cannot make the same interactions. The replacement amino acid is often alanine, which cannot form significant intermolecular interactions, but retains a similar degree of conformational restriction to other non-glycine amino acids. Another approach is to substitute relatively smaller residues with bulkier ones to cause steric clashes and thus a disruption of binding. Alternatively, the bump and hole approach (*vide infra*) uses site-directed mutagenesis to replace a relatively larger amino acid with a smaller one, creating a “hole” into which a synthetic ligand is designed to fit, allowing ligand selectivity to be manipulated.

The ability of bromodomains to bind KAc residues was first established by the Zhou and co-workers using site-directed mutagenesis studies to determine which amino acids of the bromodomain are important in this interaction.^[7b] In these studies the bromodomain of PCAF was observed to bind an histone H4-mimicking peptide (H4_[1-12]K8Ac) with a dissociation

constant (K_d) of $346 \mu\text{M} \pm 54 \mu\text{M}$, using concentration-dependent shifts in ¹⁵N-heteronuclear single quantum coherence (HSQC) spectra. Alanine scanning was used to determine relative contributions of conserved residues to ligand binding. The Y802A, Y760A and V752A mutations (Figure 1A) were found to destabilize ZA loop folding and significantly reduced ligand-binding. The Y809A mutation perturbed only a few amide resonances, but completely abrogated bromodomain binding, suggesting that this residue is important in the bromodomain-KAc interaction. X-Ray crystal structures of the bromodomain of the histone acetyltransferase Gcn5p complexed with H4_[15-29]K16Ac revealed that Y364 (corresponds to Y760 in PCAF) forms a water-mediated hydrogen bond with KAc (Figure 1B). These structural analyses provided evidence for a direct hydrogen bond of KAc to N407, which is found at the top of helix B.^[26] Alanine substitution of this highly conserved asparagine residue in several bromodomains resulted in reduced KAc binding, confirming that this amino acid is important for the recognition and binding of KAc residues by bromodomains.^[15, 27] However, it is noteworthy that there are bromodomain-containing proteins, including MLL1, which lack an asparagine or any other hydrogen bond donating residue at this position, suggesting that these bromodomains either do not bind acetylated lysine residues or have a significantly different mechanism for KAc recognition.^[28]

Later studies conducted by Philpott *et al.* employed an N140F mutation in BRD4(1) [or the equivalent N433F mutation in BRD4(2), N115F and N390F in BRD3, N981F in TRIM24, N1873F in BAZ2A, N211F in BRD7, and N808F in GCN5L2] rather than an N140A mutation. The insertion of the bulkier F residue more effectively disrupts the bromodomain-KAc interaction.^[29] This observation suggests that the highly conserved KAc-binding asparagine residue does not contribute substantially to the binding affinity of KAc (or synthetic bromodomain ligands) through enthalpic interactions, but serves to correctly orient the ligand in the binding site.

2.2. The use of mutagenesis to link acetylation with downstream activity

Before structural evidence for the recognition of KAc by bromodomains was available, *in vivo* attempts were made to link the histone acetyl transferase (HAT) Gcn5p and its acetylated products to transcriptional activation and cell growth in yeast.^[30] Mutant histone alleles, containing lysine to arginine, glycine or glutamine substitutions along the N-terminal tails, were introduced to histone-encoding genes *H3* and *H4* by plasmid shuffle. By converting lysine to the neutral amino acid glutamine Zhang *et al.* aimed to mimic KAc and bypass the need for Gcn5p, while a mutation to arginine was thought to mimic the protonated state of lysine and thus enhance defects associated with Gcn5p loss. The downstream effects of these mutations were monitored in yeast strains with and without functional *GCN5*. Mutation of H3K14, which was identified as the major target of recombinant Gcn5p acetylation *in vitro*, conferred a strong, synthetic growth defect in cells lacking functional *GCN5*, while the cells with the wild type *GCN5* were hardly affected. The common phenotype for all three of the H3K14 (Q, R and G) mutations indicated that the loss of the lysine residue is the most significant change and that the change in charge is less important than the change in structure of this residue upon acetylation. The synergistic growth defects indicated redundancies both in functions of specific acetylation events and in the enzymes that mediate these events.^[30]

2.3. The use of mutagenesis to probe the binding of small molecules to bromodomains

Mutations in the KAc binding pocket highlight interactions responsible for affinity, and can therefore guide SAR studies. Appropriate mutations can guide enhancement of ligand affinity.^[31] This approach was used to probe (+)-JQ1 (**1**) binding to BRD4. Ten conserved amino acids were selected for mutagenesis studies by Jung *et al.*,^[31a] based on interactions predicted using X-ray crystal structures.^[32] The structural integrity of the mutant proteins was confirmed by differential scanning fluorimetry (DSF), while competition time-resolved Förster resonance energy transfer (TR-FRET) and surface plasmon resonance (SPR) assays were used to monitor the ligand binding to the mutants. As expected from contributions to peptide binding, loss of affinity was observed upon N140A substitution. In addition to being involved in KAc recognition in most bromodomains, this residue is also interacts with the KAc-mimicking moiety found in most high affinity bromodomain ligands, in this case the 3-methyl-1,2,4-triazole ring of (+)-JQ1 (**1**).^[32] The Y97F mutation disrupts the water-mediated hydrogen-bond that this residue forms with (+)-JQ1 (**1**), and consequently a reduction in binding affinity was observed. Equally important for the binding of (+)-JQ1 (**1**) to BRD4 were M149 and a tryptophan residue (W81) found in the 'WPF' shelf, which forms hydrophobic interactions with the 4-chlorophenyl moiety of (+)-JQ1 (**1**). However, (+)-JQ1 (**1**) binding to the Y139F and D145A mutants was not significantly different compared with wild-type BRD4 (Figure 2A), indicating that they do not interact with this ligand.

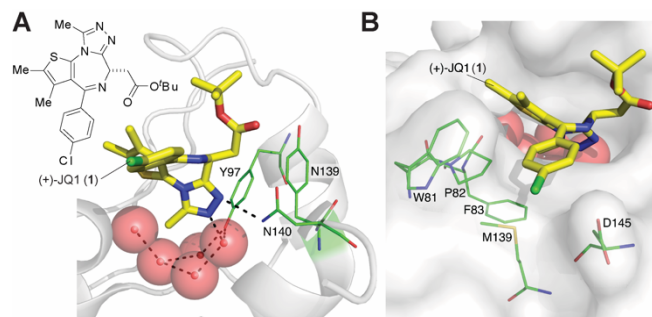


Figure 2. A) Chemical structure of (+)-JQ1 (**1**) and X-ray crystal structure (PDB ID: 3MX) showing the interactions of (+)-JQ1 (carbon = yellow) with the KAc binding pocket of BRD4(1). B) X-Ray crystal structure (PDB ID: 3MXF) showing the interactions of (+)-JQ1 (carbon = yellow) with the WPF shelf region of BRD4(1). Mutated residues are highlighted in green.

To assess the robustness of their new *in vivo* TR-FRET assay probing protein stabilization upon ligand binding, Schulze *et al.* tested the effects of point mutations in BRD4 on the binding of (+)-JQ1 (**1**) and 48 other small molecules. Comparisons were made in HEK293-6E cells between wild-type (WT) BRD4 and a set of mutants designed to disrupt well-established BRD4-ligand interactions. The EC₅₀ values for KAc ligands including (+)-JQ1, I-BET151, I-BET762, and PFI-1 were substantially increased for the Y97F, N140A, and M149A mutants, while the W81A mutant was less affected compared to wild-type BRD4 (Figure 2B).^[31c]

2.4. Probing the influence of amino acids surrounding KAc on bromodomain selectivity

It is thought that a significant degree of binding partner selectivity for bromodomains arises from interactions with amino acids proximal to the KAc residue. A high throughput AlphaScreen-based peptide displacement assay was developed by Philpott *et al.*^[33] This assay was used to screen and quantify the affinity of histone-mimicking peptides, bearing a range of PTMs, to known and suspected bromodomain binding partners. This systematic approach of screening multiple combinations of lysine and arginine modifications allowed preferential recognition patterns to be identified, and selectivity between different bromodomain proteins to be compared.^[33]

An NMR- and isothermal titration calorimetry (ITC)-based study by Ferguson *et al.*^[34] investigated the effect of individual residues of the H3_[4-25]K14Ac peptide on binding to BAZ2B bromodomain, a previously identified interaction partner.^[33] By sequentially removing amino acids on either side of K14Ac, the authors showed that residues more than five positions away from K14Ac have negligible contributions to the overall binding. Computational modelling, using HADDOCK, suggested a critical role for both R17 and K18, however, ITC experiments involving the corresponding truncated peptides only verified the importance of R17. Removal of K9 or K18 only caused a two-fold loss in affinity, without any additive effects. A negligible difference in overall binding was observed when excluding Q19.

The HIV-1 Tat protein binds to the PCAF bromodomain through K50Ac.^[35] This interaction was investigated using an alanine scan

of the three nearest arginine residues (R49A, R52A, R53A) in HIV-1 Tat. In each case R to A mutation caused only a minimal change in binding affinity, indicating that these residues are not important in this interaction. However, a significant loss of affinity was observed with Y47A or Q54A mutations of the HIV-Tat protein, providing evidence for their involvement in the bromodomain interaction.^[35b] Interestingly, in the absence of K50 acetylation, PCAF binds to residues 20–40 within HIV-1 Tat. Acetylation of K28 in the model peptide HIV-1 Tat_[23–40]K28Ac was reported to abrogate the interaction with PCAF.^[36]

Histones or histone-mimicking peptides with multiple KAc sites tend to show higher affinity for bromodomains in the BET family, compared to monoacetylated histones or peptides.^[15, 27b, 31a, 33, 37] This observation is, at least in part, explained by the BET bromodomains being capable of binding to two KAc modifications simultaneously. The diacetylated histone H4_[1–25]K5,8(Ac)₂ is an example, in which linking residues of G and C suggest the importance of flexibility between the two KAc residues.^[31a] This two-residue linker is optimal for interaction with the first bromodomain in BET family members, however, a longer spacer was also tolerated by BRD2(1). For two-residue spacers, bulky amino acids in the first spacer position were not tolerated, but changes of residue properties in the second position of the spacer did not strongly influence binding. Binding of di-KAc marks separated by a spacer of at least three amino acids, as in H4K8,16(Ac)₂ and H4K16,20(Ac)₂, required a glycine or a hydrophobic residue in the first linker position for optimal binding to the first bromodomains of the BET family. The introduction of acidic residues in any linker position led to loss of interaction with H4 histone tail peptides.^[15] Studies by Jung *et al.* suggested a major conformational impact of H4G4 and H4G9 on recognition and accessibility of di- and tetra-acetylated H4 histone peptides by BRD4(1), as an alanine exchange of these glycine residues led to a significantly reduced affinity.^[31a]

Olp *et al.* investigated how metabolically-derived, non-acetyl, lysine acylations neighboring KAc in histone H4-mimicking peptides affect the binding of the BET bromodomains. Binding of BRD2(1) and BRD4(1) to H4K5Ac was enhanced 1.4–9.5-fold by any neighboring acylation of K8 that was tested (e.g. butyryl, crotonyl, glutaryl). These results suggest a secondary H4K8Ac binding site, which is more permissive of non-acetyl acylations than previously appreciated. Conversely, C-terminal BET bromodomains showed 9.9–13.5-fold decreased binding for polyacylated compared to monoacylated H4 tails, indicating that the C-terminal bromodomains do not cooperatively bind multiple acylations.^[38] These results suggest that the cellular levels of acyl-CoA metabolites might tune or block recruitment of the BET bromodomains to chromatin, linking metabolism to bromodomain-mediated gene transcription.

2.5. Functional genomics: Correlating proteins to a specific phenotype via CRISPR Cas-9

Amongst genome editing methodologies, clustered, regularly interspaced, short palindromic repeats (CRISPR), and especially the type II CRISPR-associated protein 9 (Cas-9), has gained considerable attention over the last few years.^[39] This method has

been employed in eukaryotic cell lines both *in vitro* and *in vivo*, generating gene knock-downs, which can be used to interrogate gene function and to validate proteins as targets for the development of novel treatments.^[40] The CRISPR/Cas9 system has certain advantages over alternative genome editing tools, such as RNAi, which suffer from inadequate mRNA suppression or non-specific targeting. Unlike RNAi, which acts at the mRNA level, CRISPR/Cas9 has the ability to introduce heritable precision insertions and deletions in eukaryotic genes.^[41]

Using CRISPR/Cas-9, the BRD4-dependent nature of AML expression was demonstrated using negative selection, providing extraordinary detail on the different BRD4 domains involved. Besides the two bromodomains of BRD4, the extra-terminal (ET) domain and a C-terminal domain were also shown to be important in determining the phenotypic outcome.^[42] Another study by Mazur *et al.*, suggested a key role for p57 during dual treatment with the BET bromodomain inhibitor (+)-JQ1 and SAHA [a non-selective lysine deacetylase (KDAC) inhibitor] in pancreatic ductal adenocarcinoma (PDAC). Using a CRISPR-based assay the authors were able to verify that transcriptional induction of p57 is the key mediator of cell death in PDAC cells upon dual treatment.^[43] More recently, Gechijian *et al.* applied a CRISPR-scanning strategy^[42] in combination with a proteolysis-targeting chimera (PROTAC) approach (see section 5.4.2) to reveal that the RING domain but not the bromodomain of TRIM24 is responsible for the functional TRIM24 dependency of the leukemia cell lines MOLM-13 and MV4;11.^[44] This studies demonstrates the complementary nature of CRISPR and PROTAC technologies for investigating protein function. These initial studies indicate that CRISPR/Cas9 methodology holds great potential for identifying and validating bromodomains as future targets for therapeutic treatment.

2.6. Innovative assay technologies for identifying bromodomain ligands

2.6.1. *In vitro* assays

In vitro biophysical assays that provide detailed information on ligand affinity for bromodomains have been invaluable in the development of bromodomain ligands. This results, at least in part, from the fact that isolated bromodomains can usually be expressed and properly folded separately from the rest of the bromodomain-containing protein in which they are found.

Fluorescence polarization (FP) assays, relying on the displacement of labelled bromodomain ligands from the KAc binding site upon ligand binding, have been used in the identification of bromodomain ligands.^[22b, 45] FP assays are typically less prone to assay artefacts resulting from fluorescence interference than fluorescence-based assays. However, like all displacement assays, rely on the availability of

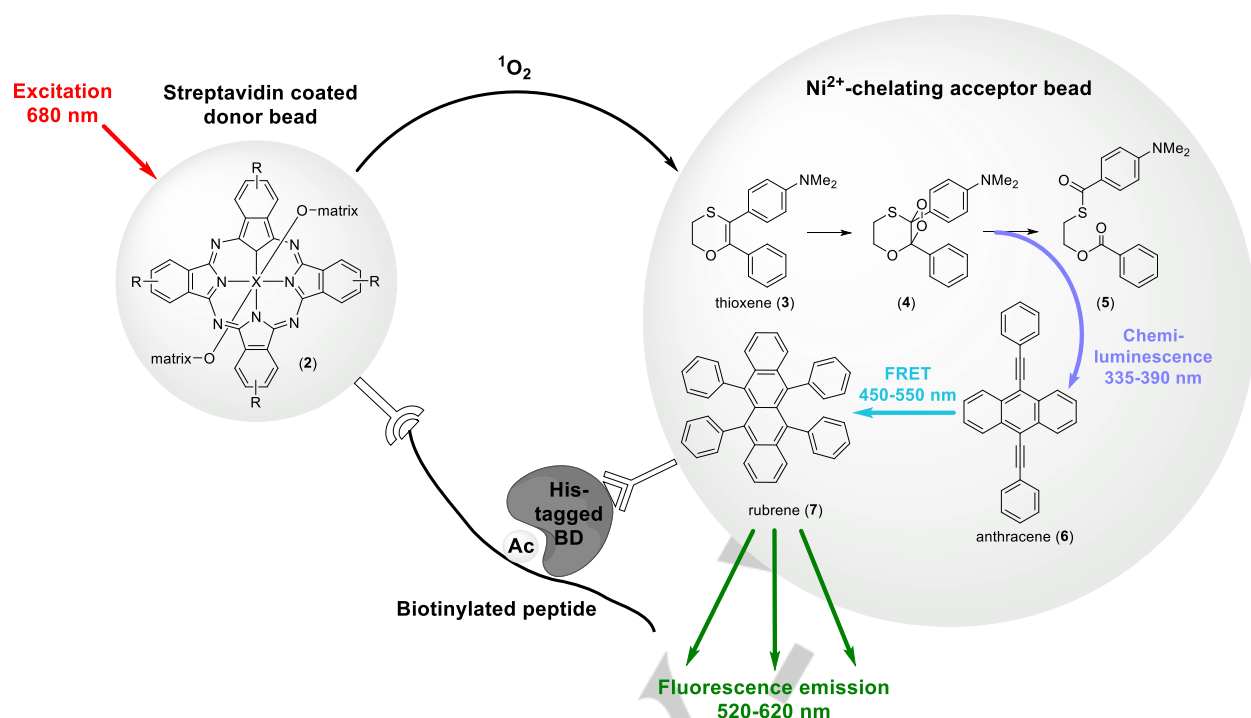


Figure 3. Cartoon representation of the AlphaScreen technology. The donor beads contain a phthalocyanine photosensitizer (**2**, chemical structure not fully disclosed by the vendor) that excites ambient oxygen to a singlet state upon irradiation at 680 nm. A chemiluminescent signal is generated within an acceptor bead, if it is located in close enough proximity to receive singlet O_2 . The singlet O_2 initially reacts with thioxene (**3**) to generate the dioxetane (**4**), which undergoes first-order decay to the diester (**5**) with a chemiluminescence emission that is transferred to anthracene (**6**) and then to rubrene (**7**) via Förster resonance energy transfer (FRET), resulting in a broad fluorescence emission from 520 nm to 620 nm.^[46] Bromodomain ligands can displace the bromodomain (BD) from the KAc(s) of the biotinylated peptide, increasing the distance between donor and acceptor bead, which hampers the transfer of singlet O_2 from donor to acceptor bead. This results in a reduction in fluorescence and allows an IC_{50} values to be determined.

a protein ligand with suitable binding affinity. The Amplified Luminescent Proximity Homogenous Assay (AlphaScreen) has been heavily used in work to identify bromodomain ligands, especially for the BET family (Figure 3).^[32, 46b, 47] While prone to false positive results and susceptible to assay interference, AlphaScreen remains a powerful high-throughput assay for initial screening of bromodomain ligands, where the endogenous cognate binding partner is known. While, absolute IC_{50} values can vary between assay runs, the affinity of compounds within a series can be ranked effectively. The AlphaScreen TruHits kit can be used to identify false positives resulting from singlet oxygen quenching or biotin mimetics.

The commercially available BROMOscan assay, provided by DiscoverX, has become the accepted gold-standard for *in vitro* selectivity screening.^[47c, 48] This high-throughput, quantitative, platform detects bromodomain binding in 40 validated bromodomain assays. Binding of a small molecule to a given bromodomain prevents the DNA-labeled bromodomains from binding to an immobilized ligand. Measuring the amount of bromodomain captured in test versus control samples, using a quantitative and ultra-sensitive qPCR method, allows the characterization of bromodomain binding over a broad range of concentrations and affinities (<100 pM to >10 μ M). This method of assay readout is less prone to compound interference compared to other displacement assays, such as FP or AlphaScreen. Label-free methods based on DSF,^[32, 47b, 47d, 49] ITC,^[32, 47b] NMR (water-LOGSY,¹⁹F-observed, and STD)^[50] have

also been established to assess binding to bromodomains. These label-free methods do not rely on the availability of previously-identified ligands, which can be especially useful when studying bromodomains for which an endogenous binding partner is not known, or for which only low affinity ligands have been identified. These approaches allow the direct determination of dissociation constants (K_d values), avoiding the problems associated with IC_{50} values, and render the development of labelled probes unnecessary. Among the label-free methods DSF offers the highest throughput, but the output is only semi-quantitative. ITC provides the most information on ligand binding including enthalpic and entropic contribution, and stoichiometry of ligand binding.

2.6.2. Assays to assess cellular target engagement

The translation of biophysical measurements directly in a cellular environment has enabled the development of several methods suitable to assess cellular target engagement. These cellular assays also allow initial insight into properties including membrane permeability and cellular stability. In the case of bromodomains, this is exemplified by the application of fluorescence recovery after photobleaching (FRAP) assays (see section 2.7),^[29, 32] time-resolved Förster resonance energy transfer (TR-FRET) assays,^[31c] cellular thermal shift assays (CETSA),^[51] and methods using bioluminescence resonance energy transfer including BRET^[52] and NanoBRET assays.^[51a, 53] Interestingly, BRET-based technologies not only give insights into cellular target engagement but also allow the residence time of

the ligand to be monitored.^[52] Unlike FRAP-, TR-FRET-, and BRET-based methods, CETSA assays do not require any protein or ligand labels and thus enable assessment of target engagement in non-transfected cells. However, antibodies for target proteins are needed to assess their stability using western blotting. The concept of CETSA has also been expanded to a proteome-wide approach using protein mass spectrometry readout. This method termed “cellular thermal profiling by mass spectrometry” is especially powerful in the minimum assumption identification of off-targets, as the use of mass spectrometry to characterize these proteins negates the need for prior identification.^[51c] However, to our knowledge this method has not been applied to bromodomain ligands yet. Photo-cross-linking probes for bromodomains (chapter 5.2) and the bromodomain-targeted PROTACs (chapter 5.4) are also useful tools to assess cellular target engagement and are discussed below.

2.7. Applications of methods for cellular target engagement in combination with mutagenesis strategies

Unlike enzymes or receptors, monitoring PPIs in a cellular environment is challenging due to the absence of readily measurable parameters for target engagement (e.g. enzyme products or ion fluxes). The use of a FRAP assay developed by Philpott *et al.* enabled the evaluation of bromodomain binding capability.^[29] GFP-labelled bromodomain-containing proteins are bleached upon exposure to an intense laser pulse, the time for the fluorescence to recover is then monitored. Without a ligand present, the bromodomain-containing proteins are associated with hyper-acetylated chromatin reducing their mobility and lengthening the recovery time. When an effective ligand for the bromodomain is present the association with chromatin is weakened, leading to greater mobility and reduced time for recovery from photobleaching. As proof-of-concept, Philpott *et al.* mutated several conserved residues in a set of 11 representative bromodomains throughout the phylogenetic tree, and analysed the effects on chromatin binding. Consistent with the literature,^[15, 27, 31a] the well-conserved asparagine residues in BRD4 (N140F/N433F), BRD3 (N115F/N390F) and TRIM24 (N981F) were identified to substantially reduce recovery times, confirming the importance of this residue for binding to acetylated chromatin. Conversely, mutations of the corresponding asparagine residue in SMARCA2 bromodomain, a central component of the SWI/SNF chromatin remodelling complex, did not affect fluorescence recovery, suggesting an alternative binding interaction, at least in the context investigated.^[29]

A key question in the function of the BET bromodomains has been whether the first bromodomain and the second bromodomain have different functions, and consequently, whether selective inhibition would result in different phenotypes. Prior to the publication of ligands that show selectivity for either the first or second BET bromodomains,^[54] Baud *et al.* took an elegant approach to address this question. To expand the current understanding of the complex processes revolving around the BET bromodomains, they engineered controlled selectivity using the “bump and hole” approach (Figure 4),^[31b] which was originally pioneered by Shokat to develop selective kinase inhibitors.^[55] A site-directed L to A mutation located in the KAc binding pocket

generates a “hole” that provides a cavity to be targeted by “bumped up” analogues of (+)-JQ1^[32] and I-BET762.^[22a] This approach resulted in between 30- and 540-fold selectivity of the bumped up inhibitor for the individual mutant, compared to the wild-type bromodomain. The FRAP-based studies revealed that blockade of BRD4(1) alone is sufficient to displace it from chromatin. This particular strategy can contribute to a deeper understanding of the individual BET bromodomains in a complex cellular context.^[31b, 56] In complementary work, Law *et al.* recently reported tetrahydroquinoline based inhibitors as novel tools to selectively target the second bromodomains present in the tandem bromodomains of the BET family, demonstrating that selectivity can also be achieved without the need to introduce mutations into the bromodomain.^[54b] Both of these studies suggest that BRD4(1)-selective ligands might show more targeted effects on gene transcription, and therefore fewer side effects, than pan-BET ligands.

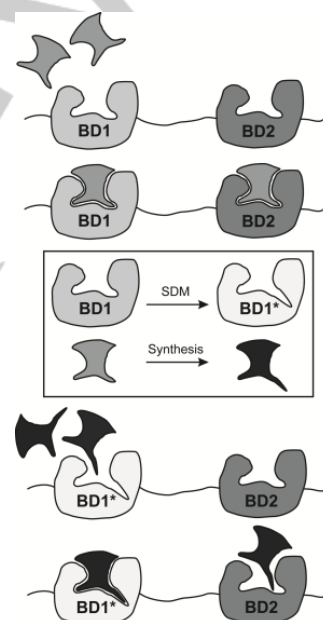


Figure 4. Cartoon representation of the “bump and hole” approach taken by Baud *et al.* to generate ligands that show selectivity for the first bromodomain of BRD4 over the second bromodomain of BRD4.^[31b]

3. The use of unnatural amino acids in the study of bromodomains

Non-proteinogenic amino acids offer the opportunity to incorporate enhanced function, structural diversity, or unnatural stereochemistry into proteins and peptides. Reprogramming of the amber stop codon to encode unnatural amino acids is a powerful method of enabling their incorporation into proteins, both *in vitro* and *in vivo*, and a constantly expanding array of functionalities.^[57] The complementary tag-and-modify approach allows labeling of reactive residues, often cysteine, to incorporate functionally useful motifs into proteins at a specified position.^[58] Such techniques have been harnessed for the study of

REVIEW

bromodomains. In ligand discovery efforts, incorporation of fluorinated amino acids into bromodomains has enabled the identification of ligand binding site and ligand binding modes, K_d values, and selectivity profiles, based on the perturbations of chemical shifts in ^{19}F NMR spectra. This approach is especially useful for bromodomains for which X-ray crystal structures have not been obtained. Incorporation of stable KAc-mimicking unnatural amino acids into histone and non-histone peptides and proteins, which do not compromise bromodomain binding, enable the precise study of KAc-mediated peptide-protein interactions.

3.1. Protein-observed NMR to study protein-ligand interactions

The use of 2D ^1H - ^{15}N HSQC NMR to characterize protein-ligand binding events for fragment-based drug discovery was first reported by Shuker *et al.* in 1996,^[59] and is a powerful tool to aid ligand discovery. Protein-observed NMR was used in some of the earliest bromodomain ligand-discovery efforts, and has been employed to identify fragments that bind to the PCAF,^[60] CREBBP^[61] and BET^[53a, 62] bromodomains. This method allows quantification of the, often low, binding affinities for fragments, and can provide detailed structural information regarding the location of ligand binding sites. However, long acquisition times, the requirement for high protein concentrations, and detailed resonance assignments can limit the throughput possible using this approach.^[63] In recent years, protein-observed ^{19}F NMR (PrOF NMR) has been adopted in fragment-based screening efforts for the characterization of ligand binding at PPI sites,^[64] and has also provided insights into protein folding and conformational dynamics.^[64c, 65] The 100% naturally abundant, spin $1/2$ ^{19}F isotope has a signal sensitivity of 83%, relative to ^1H , and is affected by changes in the local van der Waals environment and electrostatic fields.^[65a] The relatively fast acquisition times and low protein concentration required (40–50 μM) make this a suitable approach for ligand screening studies. In addition, the incorporation of fluorine into an amino acid sequence only leads to a modest perturbation in the tertiary protein structure, due to the similarity of the van der Waals radii of fluorine and hydrogen (1.47 Å and 1.20 Å, respectively).^[66] PPI interaction sites are often enriched in aromatic amino acid residues,^[67] including interfaces involving loops,^[68] α -helices^[69] and β -sheets.^[70] Consequently, aromatic residues (Phe, Trp and Tyr) are generally chosen for ^{19}F labelling (Figure 5). Additionally, they have low abundances in protein structures, reducing the complexity of assignment, and the number of fluorinated residues introduced into the target protein.^[71] Biosynthetic incorporation using auxotrophic cell lines to selectively replace a given native amino acid with the corresponding fluorinated variant has been one of the main strategies for ^{19}F labelling of proteins.^[72] Alternative strategies include site-specific incorporation of fluorinated amino acids into proteins through the use of an orthogonal amber suppressor tRNA/aminoacyl-tRNA synthetase pair,^[73] and post-translational chemical modification of protein side chains, usually thiol or amino groups, with fluorinated tags, although these approaches have not been applied to bromodomains to date.^[65b, 74] Sequence assignment of the fluorinated proteins are often completed through systematic site-directed mutagenesis, with the

disappearance of ^{19}F NMR resonance corresponding to the replaced residue.^[71] Moderate to high conservation of aromatic amino acids is observed near to histone binding sites in the sequence analyses of all 61 bromodomains,^[15] making PrOF NMR an ideal approach for identifying new tool molecules in this field.^[75]

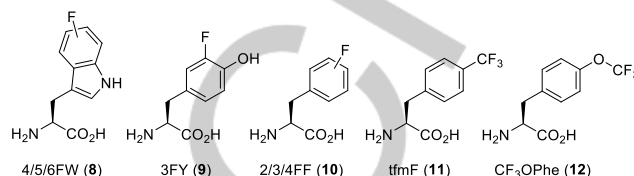


Figure 5. Examples of fluorinated aromatic residues utilized in ^{19}F NMR studies of biological systems as reviewed in Arntson *et al.*,^[71] 4/5/6-fluorotryptophan (4/5/6FW; 8), 3-fluorotyrosine (3FY; 9), 2/3/4-fluorophenylalanine (4/5/6FF; 10), 4-(trifluoromethyl)phenylalanine (tfmF; 11), 4-trifluoromethoxy-phenylalanine (CF₃OPhe; 12).

3.2. The use of protein-observed fluorine (PrOF) NMR studies to investigate bromodomain ligand binding modes

Mishra *et al.* employed PrOF NMR to characterize the binding footprints and dissociation constants (K_d) of small, weakly-binding, ligands for BET (BRD4 and BRDT) and non-BET (BPTF) bromodomains.^[75a] The N-terminal bromodomain of BRD4 [BRD4(1)] was labelled with either 5-fluorotryptophan [5FW (8), Figure 5], at positions W75, W81 and W120, or 3-fluorotyrosine [3FY (9)], at positions Y65, Y97, Y98, Y118, Y119, Y137 and Y139. Labeling was achieved by replacement of the naturally-occurring amino acids with the corresponding fluorinated analogue in the media. These amino acid residues were chosen for fluorine-labelling as they are located proximal to the known binding site of the pan-BET bromodomain ligand (+)-JQ1 (1, Figure 6A). Circular dichroism (CD), ITC, and X-ray crystallography, showed only a minor effect on the structure and function of BRD4(1) upon incorporation of the fluorinated amino acids. Resonance assignments were made using site-directed mutagenesis and ligand binding experiments. The 5FW- and 3FY-labelled BRD4(1) ^{19}F NMR spectra displayed resonances spanning over 2 ppm (for three 5FW resonances) and 12 ppm (for seven 3FY resonances), respectively (Figure 6B). This large chemical shift range also implies that the protein is properly folded, due to the sensitivity of fluorine towards non-covalent tertiary structure interactions.^[65a] The binding site location can be estimated based on the perturbation of these resonances due to the responsiveness of the fluorine chemical shifts towards ligand binding. For example, residues W81, Y97, Y98 and Y139 are located within the binding site of (+)-JQ1 (Figure 6A) and these resonances undergo a slow exchange process as a result of (+)-JQ1 binding. This results in a broadened and left-shifted resonance of W81 upon titration with (+)-JQ1. However, for

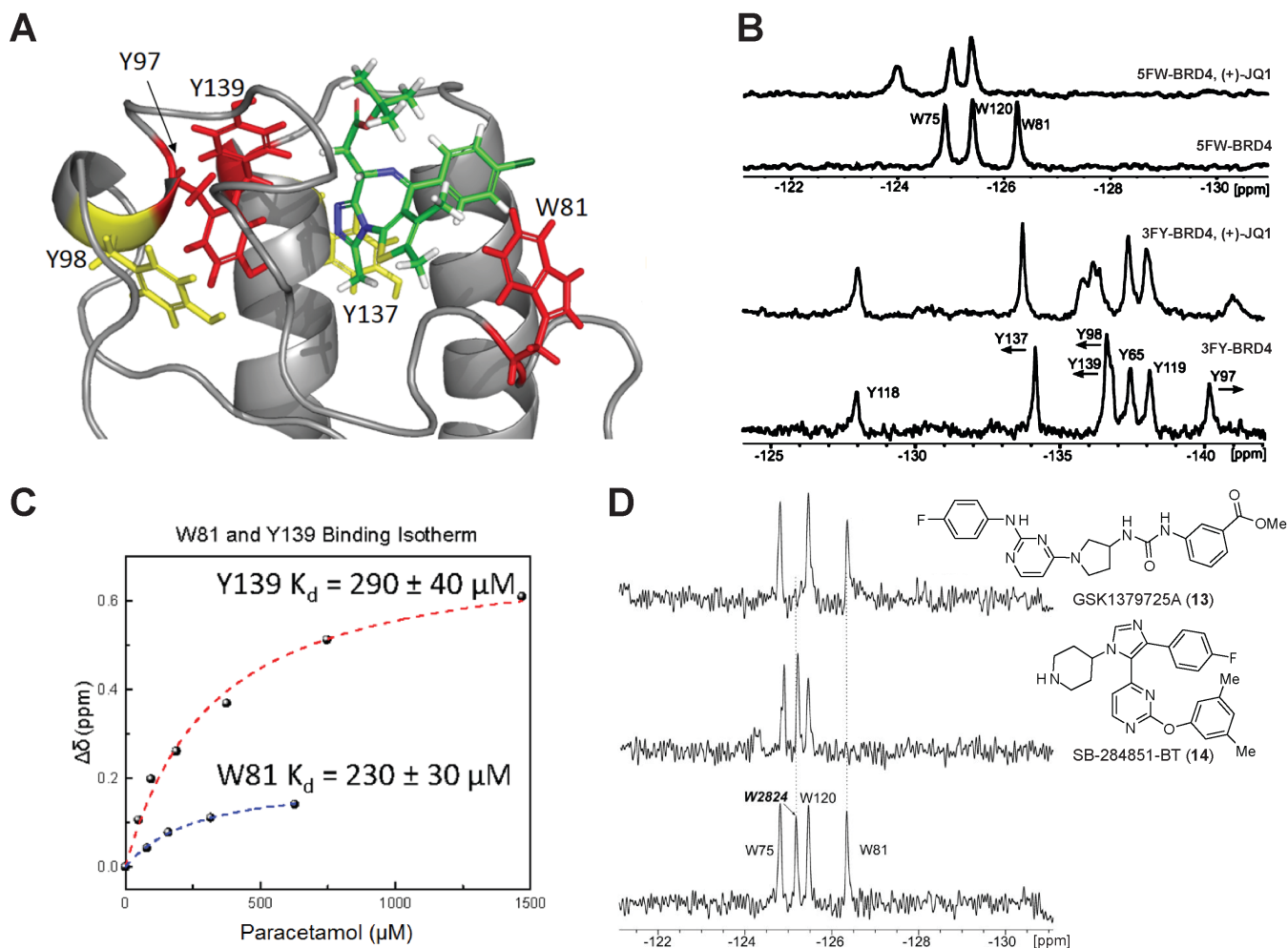


Figure 6. A) Cartoon diagram of BRD4(1) in complex with (+)-JQ1 (PDB ID 3MXF, carbon: green). Tyrosine (Y97, Y98, Y137, Y139) and tryptophan (W81) residues in close proximity to the (+)-JQ1 binding site. Aromatic side chains within 5 Å and 10 Å are shown in red and yellow, respectively. B) ^{19}F NMR spectra displaying the titration of (+)-JQ1 with 5FW- (top) and 3FY-BRD4(1) (bottom). Slow exchange binding is detected for resonances W81, Y97, Y98 and Y137, as the intensity of the free BRD4(1) signal disappears and a new broad signal is observed for (+)-JQ1 bound BRD4(1). C) Binding isotherms for the titration of paracetamol with 3FY- and 5FW-BRD4(1). K_d values for paracetamol are estimated based on the chemical shift perturbation of Y139 (red) and W81 (blue). D) Simultaneously detected ^{19}F NMR spectra of 5FW-BRD4(1) and 5FW-BPTF bromodomains. Perturbation of W2824 of BPTF in the presence of the BPTF selective ligand GSK1379725A (**13**, top); perturbation of W81 of BRD4(1) in the presence of the BRD4(1) selective ligand SB-284851-BT (**14**, middle); spectra in the absence of ligand (bottom). Figure 6A–C adapted with permission from Mishra *et al.*^[75a] Copyright (2014) American Chemical Society. Figure 6D adapted with permission from Urlick *et al.*^[75b]

residues W75 and W120, the resonance signals are less affected as they are located distal to the (+)-JQ1 binding site (Figure 6B).^[75] The resonance perturbation can be used to estimate K_d values, in the nanomolar to micromolar range, by titration of a ligand into the protein solution and subsequent analysis of the magnitude of chemical shift change between the bound and unbound state.

3.3. The use of protein-observed fluorine (ProOF) NMR for bromodomain ligand screening

Fragment screening using ProOF NMR has been applied to identify novel tool compounds in ligand discovery efforts for the BET bromodomain-containing proteins.^[64a, 64b, 75b] Paracetamol (acetaminophen), a fragment-like molecule that co-crystallizes with BRD2(1),^[62] could not be detected using fluorescence anisotropy or TR-FRET-based assays^[62] due to its weak affinity

for the BET bromodomains. However, ProOF NMR detected binding of paracetamol at concentrations down to 47 μM , based on the resonance perturbation for Y139 of 3FY-BRD4(1). Titration of paracetamol with 5FW-BRD4(1) and 3FY-BRD4(1) gave K_d values of 230 μM and 290 μM , respectively (Figure 6C).^[75a] A similar approach has also been applied to validate and characterize fragment binding to 5FW-BRDT(1)^[76] and to the 3FY-labelled KIX domain of CREBBP.^[64b]

The strong cellular phenotype exhibited by the BET bromodomains means that selectivity over this class of proteins is particularly important when developing ligands for non-BET bromodomains, but detection of weakly binding ligands (targeted at other proteins) is difficult. Using ProOF NMR, Urlick *et al.* screened 229 compounds from a published kinase inhibitor set (PKIS I and II) against BRD4(1) and BPTF bromodomains, simultaneously, to identify selective ligands while increasing the screening throughput.^[75b] Tryptophan residues contained within

each bromodomain were replaced with 5FW (**7**); W120, W81 and W75 for BRD4(1), and W2824 for BPTF, which is the analogous residue for W81 in BRD4(1). The perturbations of the corresponding resonances revealed the binding interactions between the evaluated ligands and the selected bromodomains (Figure 6D). This screen identified 1,2,5-oxadiazoles and arylurea-containing 2,4-disubstituted pyrimidines as new ligand classes for both bromodomains. The arylurea GSK1379725A (**13**) was identified as the first selective ligand for BPTF over BRD4, with a determined BPTF K_d value of 2.8 μ M. No binding to BRD4(1) was detected. Additionally, six ligands from the PKIS library were found to be selective for BRD4 over BPTF, including the 1,4,5-trisubstituted imidazole SB-284851-BT (**14**), which has a K_i of 310 nM. A full selectivity panel was not reported for these ligands, however, this study has set the precedent for the simultaneous screening of multiple bromodomains to aid the discovery of novel selective inhibitors. The bromodomain-binding affinity of all hits was validated using fluorescence anisotropy, and ITC experiments with non-fluorinated proteins.

3.4. Acetyl-lysine mimicking unnatural amino acids

The study of the effects of lysine acetylation at a given site in a protein requires the production of a homogenously-modified derivative of the protein of interest. The dynamic nature of the KAc mark means that the native mark itself cannot be used in such studies. Consequently, the use of unnatural amino acids that mimic KAc has been investigated, and some of these analogs are stable to the action of KDACs, which remove the KAc mark. A multitude of reports on unnatural KAc mimics were focused on the study of deacetylase enzymes.^[77] By comparison, fewer unnatural amino acids have been used to probe bromodomains (Figure 7A). Jamonnak *et al.* used an *in vitro* GST-bromodomain pull-down assay^[78] to demonstrate that methanesulfonyl-lysine (**15**) substituting K382 in human p53 could replace KAc in the recruitment of the CREBBP bromodomain without compromising the binding affinity.^[79] The methanesulfonyl-lysine-modified protein was also shown to be a weak inhibitor in KDAC8 and SIRT1 deacetylase assays, functioning as a non-hydrolysable KAc surrogate for bromodomain binding. In 2010, Huang *et al.* reported the preparation of methylthiocarbonyl-thialysine (**16**, MTCTK), a thiocarbamate analogue of KAc, using methylthiocarbonyl-aziridine (MTCA) as a quantitative and selective reagent for cysteine alkylation of peptides.^[80] MTCTK substitution of H4 acetylated tails at either K5 or K8 positions were able to compete in GFP-BRDT(1) pull down assays, however, the MTCTK modified H4 tails were found to be 2–4 fold less efficient than the native KAc-containing peptide. Nevertheless, MTCTK was shown to mimic KAc-BRDT(1) binding interactions, be recognized by site-specific anti-KAc antibodies on H3 histone proteins, and was resistant to hydrolysis by KDAC8 deacetylases. The 3,5-dimethylisoxazole motif has been employed as the KAc mimic in a large number of ligands for both the BET^[23c, 81] and CREBBP bromodomains.^[82] Sekirnik *et al.* investigated whether this group would function as a KAc mimic when incorporated into peptides and proteins.^[83] Ten isoxazole-containing amino acids were synthesized and shown to bind in a dose-dependent manner to at least one of the BRD4(1), BAZ2A or BRD9 bromodomains.

Three of these amino acids (**17–19**) were then incorporated into a histone-H4-mimicking peptide at positions K5, K8, K12 or K16, and it was shown that these peptides were able to bind to BRD4(1), with a higher affinity shown when the unnatural amino acid was incorporated at K12. Some K12-modified peptides, with K5,8,16Ac, showed higher affinity for BRD4(1) than the corresponding tetra-acetylated histone H4-mimicking peptide. In a complementary approach, it was demonstrated that an isoxazole-based alkylating agent (**20**) selectively modified cysteine residues in a histone-H4-mimicking peptide, and a K18C mutant of the complete histone H3 protein (Figure 7B). These approaches will allow the generation of homogenously-modified peptides and proteins to aid the study of protein post-translational modification in epigenetic processes.

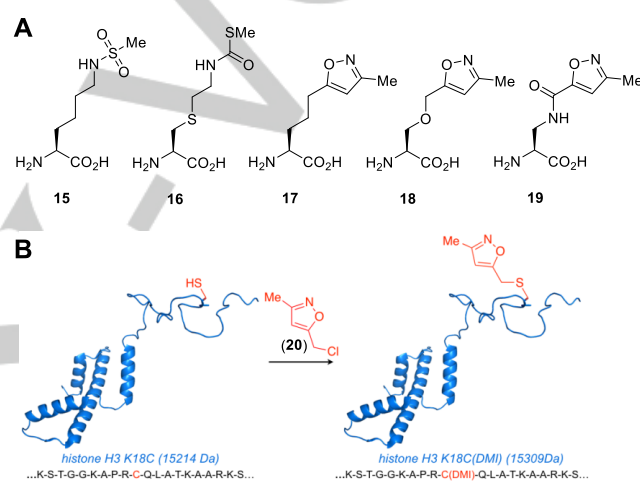


Figure 7. A) KAc mimics (**15–19**) used to study bromodomains.^[79–80, 83] B) Use of a 3,5-dimethylisoxazole-based alkylating agent (**20**) to introduce a KAc mimic onto a specific cysteine residue in the K18C mutant of histone H3.^[83]

4. Fragment-based approaches to the discovery of potent and selective bromodomain ligands

Fragment-based drug discovery (FBDD) typically involves screening a relatively small library (c. 1000 members) of low molecular weight compounds (usually < 250 Da) to identify molecules that bind a given protein with high ligand efficiency [LE = 1.37(pIC₅₀/HA) where HA = heavy atom count].^[84] While there is some discussion in the literature surrounding the thermodynamic validity of using LE,^[85] it is a useful parameter for identifying low molecular weight molecules that make efficient interactions with proteins (i.e. all or most of the heavy atoms make a contribution to ligand affinity).^[86] The use of low molecular weight fragments allows sampling of a greater proportion of chemical space than an equivalent sized library of lead-like molecules.^[87] The low binding affinity of fragments has previously been a limitation to this approach, requiring bespoke techniques for their study, however, this has largely been overcome through the use of NMR-based methods (*vide supra*), and the ready availability of X-ray co-crystal structures in many cases.^[84] A

REVIEW

fragment hit is developed into a drug-like molecule using techniques including fragment linking, merging or growing. In addition to preserving high LE, ligand lipophilic efficiency (LLE = $\text{pIC}_{50} - \text{clogP}$ or $\text{pIC}_{50} - \text{clogD}$) is typically monitored to ensure that affinity gains are attributed to high quality, specific interactions, as opposed to non-specific lipophilicity, which can result in promiscuous compounds or unwanted off-target toxicity.^[88] An LLE value of >6 is generally considered optimum for drug molecules.

The BET family of bromodomains rapidly emerged as suitable targets for a fragment-based approach, and consequently this is an area that has been well explored^[62, 89] and reviewed.^[16, 23d, 90] FBDD has also been applied to non-BET bromodomains, and, high affinity, selective ligands resulting from this approach have been published for the ATAD2,^[91] TRIM24,^[92] CREBBP,^[93] BAZ2,^[94] BRPF1,^[53c, 92] PHIP(2),^[95] BRD9,^[53a, 96] and BRD7/9 bromodomains (examples shown in Figure 8).^[48c, 97]

Two examples of fragment-based approaches to bromodomain ligand design for BET bromodomains and ATAD2, respectively, are described below, with particular focus on the fragment approaches utilized.

4.1. Benzo[b]isoxazole[4,5-d]azepines and benzotriazolo[4,3d][1,4]diazepines as potent and selective BET bromodomain ligands

Scientists from Constellation Pharmaceuticals reported the optimization of aminoisoxazole fragment **29** to give the nanomolar BET ligand, CPI-3 (**31**).^[47d] Fragment **29** ($\text{IC}_{50} = 33 \mu\text{M}$) was identified using a fragment screen, and was shown to act as an acetyl lysine (KAc) mimic by X-ray crystallography. This fragment shows high ligand efficiency (LE = 0.47), acceptable lipophilic ligand efficiency for a fragment (LLE = 2.74) and is consequently a good starting point for FBDD. On the basis of the crystallographically-observed binding mode, it was proposed that merging the fragment with the scaffold of known high affinity BET bromodomain ligand, (+)-JQ1 (**1**), $\text{IC}_{50} = 24 \text{ nM}$,^[32] could result in a superior ligand. The aim was to retain the shape and interactions of (+)-JQ1, but exploit the isoxazole as a KAc mimic, which had been previously used in other ligands.^[47a, 49] This fragment merge generated compound **30** and is an example of the fragment-based approach being complementary to other ligand discovery techniques, in this case phenotypic screening. As is typical with fragment merging, the resulting ligand suffered a drop in affinity, with **30** showing a BRD4(1) IC_{50} value of 290 nM, LE of 0.29, and LLE of 0.58 (Table 1). Optimization of the *tert*-butyl ester side chain led to an understanding of a structure-activity relationships (SAR) for this region, and identification of compound **31**, which incorporates a primary amide in this position. This ligand has a BRD4(1) IC_{50} value of 26 nM and thermal shift (ΔTm) of 10.10 K.

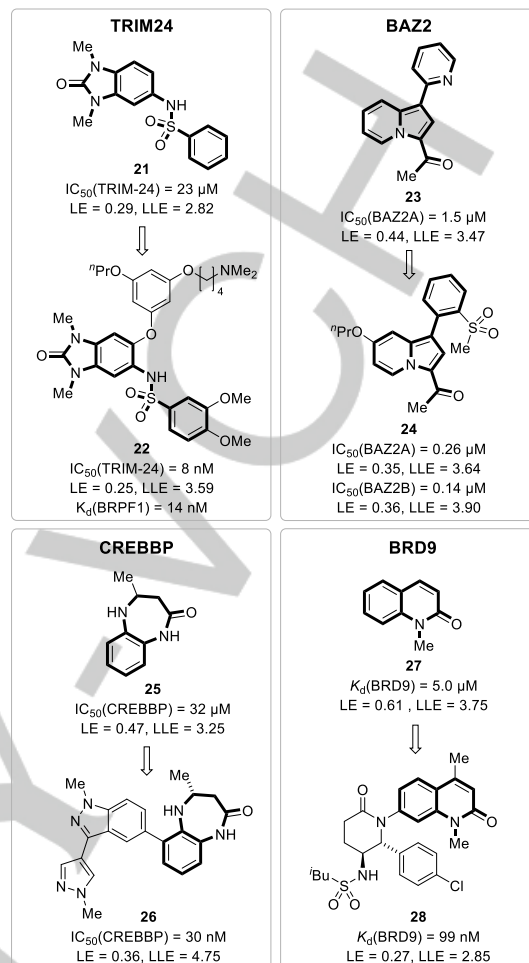


Figure 8. Example bromodomain fragment hits and elaborated ligands (**21–28**) for low druggability bromodomains, affinity data,^[92, 93c, 94, 97] ligand efficiency (LE), and ligand lipophilic efficiency (LLE) values are given. The original fragment scaffold is highlighted in bold. In all cases shown this includes the KAc-mimicking group.

This modification led to ligand efficiency being recovered (LE = 0.38) and a significant improvement in lipophilic ligand efficiency (LLE = 4.27). Subsequent exploration of the WPF shelf by variation of the chloroaromatic ring did not lead to increased affinity for BRD4(1). Compound **31** also exhibited good selectivity over non-BET bromodomains in a thermal shift assay, with the next highest ΔTm being 0.58 K for BRD7, although appropriate caution should be exercised when using thermal shift to estimate ligand selectivity. Like most other BET-selective bromodomain inhibitors, **31** gains significant affinity and selectivity from hydrophobic interactions between the 4-chlorophenyl ring and the WPF shelf. This region is conserved in all BET bromodomains, but not found in any other human bromodomains. Compound **31**, CPI-3, was subjected to preliminary biological assays and *in vivo* testing in mice. These studies revealed that **31** is an orally-bioavailable BET bromodomain ligand, which is capable of blocking MYC mRNA expression *in vivo* in a dose-dependent manner.^[47d] To improve the ADME properties of **31**, especially the

metabolic stability, the ligand was stripped back to the core fragment **32** (IC_{50} = 30 μ M, LE = 0.41).^[98] Exchange of the thiophene for an unsubstituted aryl ring eliminated possible thiophene-linked metabolic issues including S-oxidation and epoxidation.^[99] Scaffold hopping from an imine- (**31**) to an aniline-based (**32**) scaffold was predicted to retain the overall shape of the ligand while providing a different metabolic profile for the series. Compound **32** was subjected to a fragment growing strategy, with identification of the 4-cyanoaryl substituent on the 6-position nitrogen as optimal, giving compound **33** with affinity of 550 nM. Ligand efficiency and lipophilic ligand efficiency were largely preserved, despite a significant increase in lipophilicity. Further SAR on the aromatic 8-position and the aliphatic 4-position led to identification of a class of potent ligands, exemplified by compound **34**, however, these compounds showed unacceptable *in vitro* clearance properties. Larger groups at the 4-position were detrimental to affinity, in contrast to structurally similar ligands where far larger groups are tolerated (*c.f.* (+)-JQ1). The high lipophilicity of the 5,6-dihydro-4*H*-benzo[*b*]isoxazolo[4,5-*d*]azepine structure and the unfavorable *in vitro* clearance properties of this series inspired a further scaffold hop by replacement of the isoxazole moiety, which was been implicated with poor metabolic stability,^[100] with the more polar triazole.

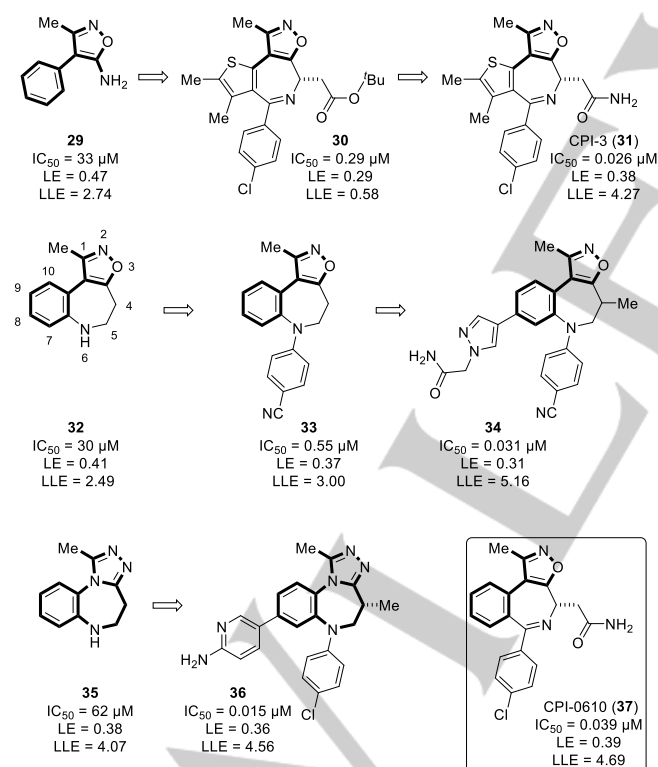


Figure 9. Outline of the optimization conducted on fragment **29** to give the BET bromodomain ligand **36** and CPI-0610 (**37**).^[47d, 98, 101] Reported affinity data (IC_{50}), ligand efficiency (LE), and ligand lipophilic efficiency (LLE) values are given for the interaction with BRD4(1). The original fragment scaffold is highlighted in bold.

Analogous SAR performed on this fragment, **35** (IC_{50} = 62 μ M, LE = 0.38), identified ligand **36** as a high affinity ligand with an IC_{50} value of 15 nM. The highest off-target affinity is to CREBBP (IC_{50} = 2.2 μ M) giving 147-fold selectivity, with higher selectivity seen over the other bromodomains evaluated. The presence of the chlorophenyl, as opposed to the cyanophenyl, negated the beneficial logP decrease from the heterocycle swap, leading to a more lipophilic ligand family. Despite this, liver clearance was improved. Further *in vivo* testing indicated sufficiently favorable ADME properties for oral administration, with modulation of IL-6 levels in a dose-dependent manner (IL-6 EC_{50} = 13 nM).^[98] Additional routes for the optimization of fragment **29** led to the benzoisoxazoloazepine CPI-0610 (**37**, Figure 9).^[101] It is notable that the original fragment forms the core of the ligand (Figure 9). This compound shows >380-fold selectivity for the BET bromodomains, possesses good oral bioavailability, and is currently in two Phase 1 and two Phase 2 clinical trials for the treatment of cancers, including malignant peripheral nerve sheath tumor, lymphoma, multiple myeloma, and leukemia.^[24]

Table 1. BET fragment optimization, with published affinity data.^[47d, 98, 101] Red indicates low IC_{50} values, and green indicates high IC_{50} values.

Cmpd	BET IC_{50} ^[a]	cLogP ^[b]	cLogD _{pH7.4} ^[b]	LE ^[c]	LLE ^[d]
29	33 μ M	1.74	2.14	0.47	2.74
30	0.29 μ M	5.96	5.69	0.29	0.58
31	0.026 μ M	3.32	3.29	0.38	4.27
32	30 μ M	2.03	2.53	0.41	2.49
33	0.55 μ M	3.26	3.80	0.37	3.00
34	0.031 μ M	2.35	2.97	0.31	5.16
35	62 μ M	0.14	0.88	0.38	4.07
36	0.015 μ M	3.26	2.70	0.36	4.56
37	0.039 μ M	2.72	2.78	0.39	4.69

[a] BET family potency characterized by BRD4(1) IC_{50} . [b] cLogP and cLogD_{pH7.4} values were calculated using ACD/Labs I-Lab 2.0 software (Algorithm Version: 5.0.0.184). [c] Ligand efficiency calculated as $LE = 1.37(pIC_{50}/HA)$ where HA is heavy atom count. [d] Ligand lipophilic efficiency calculated as $LLE = pIC_{50} - clogP$

4.2. Naphthyridones as potent and selective ATAD2 ligands

Scientists at GSK used a FBDD approach to develop the first potent and selective ATAD2 bromodomain ligands.^[91a-c] While fragment hits for ATAD2 had previously been identified but not elaborated into ligands,^[102] optimization of a quinolinone fragment hit (**38**) produced a series of high affinity ligands, exemplified by compounds **46–48** (Figure 10). Compound **48** has an IC_{50} value of 50 nM for ATAD2, and 150-fold selectivity over other bromodomains, including the BET family (*c.* 500-fold), facilitating selective studies of the function of the ATAD2 bromodomain (Table 2).^[91c]

The quinolinone-based fragment **38** (IC_{50} >1 mM, LE <0.34) was identified through screening a focused library using a TR-FRET

REVIEW

assay. The compound library contained known KAc mimics, but was diversified to ensure wide coverage of chemical space. This initial fragment hit was subjected to a fragment growing strategy, which identified a tertiary amine sidechain on position 8 (**39**) as increasing ligand affinity ($IC_{50} = 100 \mu M$). A co-crystal structure indicated that this increased affinity results from the tertiary amine binding to a negatively-charged pocket formed by ATAD2 helix C.^[91a] This interaction maintained LE between **38** and **39**, while increasing LLE (LE = 0.30, LLE = 2.58), due to the increased polarity of **39** ($cLogD_{pH7.4} = -0.36$). A scaffold hop to the analogous naphthyridinone core (**40**) was then performed for synthetic convenience, however, this resulted in a drop in affinity, and consequent lower ligand efficiency ($IC_{50} = 500 \mu M$, LE = 0.25). Affinity was recovered by constraining the amine sidechain into a cyclic motif, exemplified by compound **41** ($IC_{50} = 16 \mu M$, LE = 0.37), with LE now exceeding that of the initial fragment. This was also the first ligand identified with greater affinity for ATAD2 than BRD4 ($IC_{50}[BRD4(1)] = 40 \mu M$). An investigation of the SAR at the 5-position of piperidine derivative **42** ($IC_{50} = 13 \mu M$, LE = 0.35) was undertaken to probe a pocket visible in the ATAD2 crystal structures for potential hydrogen bonding interactions. A screen of aromatic and heteroaromatic rings identified a 3-pyridyl substituent, increasing both the ATAD2 bromodomain affinity and selectivity over BET bromodomains, while maintaining ligand efficiency. A substituent screen identified a 5-position methyl group as optimum substitution on the pyridyl ring (**43**); this compound has an ATAD2 bromodomain IC_{50} value of $1.3 \mu M$, 2-fold selectivity over BRD4(1), $clogP$ of 2.95, and ligand efficiency of 0.31. This series of compounds was also cell permeant. Use of the ligands as tool compounds was, however, limited due to relatively low affinity and low selectivity over the BET bromodomain-containing proteins.^[91a]

To improve affinity and selectivity for the ATAD2 bromodomain over the BET bromodomains in particular, Bamborough *et al.* aimed to target the RVF residues of ATAD2, which are equivalent to the WPF shelf found in the BET bromodomains. Substitution at the 3'-position of the piperidine ring (**42**) was identified as a suitable vector to target this region, using X-ray crystallography. Screening a library of 3'-position derivatives of **42** identified the cyclohexyl derivate **44**, which shows improved affinity but lower selectivity for ATAD2, and decreased LLE, suggesting that the affinity gain results from lipophilic interactions (LE = 0.28, LLE = 2.07). To recover solubility and gain selectivity over the BET bromodomains, negative polarity was introduced in the form of a cyclic sulfone that was designed to interact with the arginine residue of the RVF motif. The sulfonyl derivative **45** showed decreased lipophilicity ($clogP = 0.37$), high affinity for the ATAD2 bromodomain ($IC_{50} = 790 \text{ nM}$, LLE (5.73) and 16-fold selectivity for the ATAD2 bromodomain over the BET family. An X-ray crystal structure of **45** bound to the ATAD2 bromodomain revealed that the sulfonyl group forms H-bonding interactions with Arg1007 of the RVF shelf and with Arg1077. Combination of the most favorable 3'- and 5-position substituents resulted in compound **46**, which has an ATAD2 IC_{50} value of 130 nM , 126-fold selectivity over BRD4(1) and a 40-fold selectivity over all BET bromodomains, LE of 0.26 and LLE of 5.15. This compound displayed low artificial membrane permeability, which is consistent with its low lipophilicity ($clogP = 1.75$), and efforts were required to make the compound more permeable. Methylation of the piperidine nitrogen (compound **47**) led to sufficient increase in

cell permeability, and increased selectivity over BET bromodomains but at the cost of ATAD2 bromodomain affinity ($IC_{50} = 310 \text{ nM}$, LE = 0.24, LLE = 4.36, selectivity c. 250-fold over BRD4(1) and 158-fold over all BET bromodomains). Both compound **46** and **47** were subjected to preliminary biological characterization. Binding constants (K_d) were confirmed against the ATAD2 bromodomain using surface plasmon resonance (SPR) as 80 nM and 200 nM , respectively. The selectivity of **47** over the other bromodomains was evaluated using a BROMOscan panel, indicating good selectivity of c. 400-fold over BET bromodomains, critical to application as a useful tool ligand.^[91b] Ultimately, compound selectivity and permeability were further improved by using the CF_2 group as a sulfone bioisostere and controlling the conformation of the piperidine ring by means of 1,3-interactions between the alkoxy oxygen and the protonated piperidine nitrogen. This 1,3-strain destabilizes the putative tri-axial conformation, disfavoring binding to BET, with limited impact on the tri-equatorial conformation seen in ATAD2 co-crystal structures. This dual approach culminated in **48**, the first low-nanomolar ($IC_{50} = 50 \text{ nM}$), selective [c. 500-fold over BRD4(1)], and permeable ATAD2 bromodomain ligand.^[91c] Attempts to further stabilize the tri-equatorial conformation of the piperidine ring using 2-carbon-bridged piperidine (tropane) derivatives did not yield in ATAD2 ligands with increased affinity or selectivity.^[103] Again, the original fragment hit is incorporated as the core of the final ligand, indicating that this approach allowed the identification of key ligand-protein interactions.

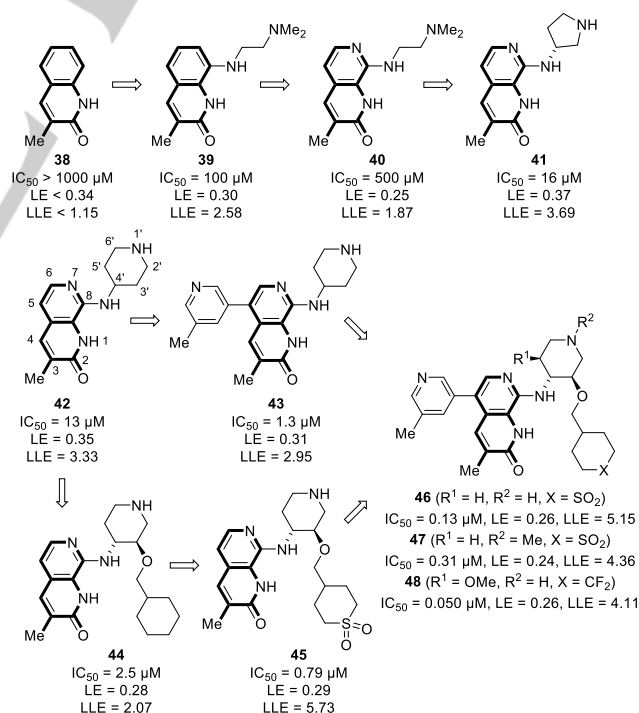


Figure 10. Structural outline for optimization of fragment **38** into ligand **48**.^[91a-c] The original fragment scaffold is highlighted in bold.

Table 2. ATAD2 fragment optimization, with published affinity data.^[91a-c] Red indicates low IC₅₀ values, and green indicates high IC₅₀ values.

cmpd	ATAD2 IC ₅₀	BET IC ₅₀ ^[a]	cLogP ^[b]	cLogD _{pH7.4} ^[b]	LE ^[c]	LLE ^[d]
38	>1000 μM	40 μM	1.85	1.82	< 0.34	< 1.15
39	100 μM	25 μM	1.42	-0.36	0.30	2.58
40	500 μM	500 μM	1.43	-0.94	0.25	1.87
41	16 μM	40 μM	1.11	-0.25	0.37	3.69
42	13 μM	4.0 μM	1.57	-1.57	0.35	3.33
43	1.3 μM	2.5 μM	2.95	-0.78	0.31	2.95
44	2.5 μM	4.0 μM	3.53	0.94	0.28	2.07
45	0.79 μM	13 μM	0.37	-0.85	0.29	5.73
46	0.13 μM	16 μM	1.75	0.09	0.26	5.15
47	0.31 μM	79 μM	2.14	1.5	0.24	4.36
48	0.050 μM	32 μM	3.19	2.82	0.26	4.11

[a] BET family affinity characterized by BRD4(1) IC₅₀. [b] cLogP and cLogD_{pH7.4} values were calculated using ACD/Labs I-Lab 2.0 software (Algorithm Version: 5.0.0.184). [c] Ligand efficiency calculated as LE = 1.37(pIC₅₀/HA) where HA is heavy atom count. [d] Ligand lipophilic efficiency calculated as LLE = pIC₅₀ – clogP

The examples outlined above show that FBDD, combined with structural studies, result in high affinity ligands with favorable properties for use as probes, and lead compounds for further development.

5. Functional probes applied to the study of bromodomains

Much work in the bromodomain area has focused on the development of lead-like chemical probes, such as those discussed in Section 4. These compounds enable the function of a given bromodomain to be assessed and represent a good starting point for drugs targeting the relevant bromodomain and, several probe compounds have been progressed to clinical trials.^[104] A second class of chemical probes exist that have been equally important in understanding bromodomain function, but which are not generally intended for development into drugs. Included in this class are affinity- and photo-affinity probes, covalent bromodomain ligands, and bifunctional, including PROTACs. This class of probe molecules are discussed below.

5.1. Affinity probes for bromodomains

Affinity probes comprise a ligand for the target protein conjugated to a chemical entity that can covalently link to the relevant protein. Inclusion of a functional tag (e.g. an alkyne or azide) allows pull-down of the bound protein(s) via attachment to biotin, or similar. Such probes enable proteomic studies to identify cellular interaction partners of the ligand. As this technology enables the relatively unbiased identification of off-targets in addition to the desired target protein, it is an essential element of cellular target validation. Examples of where this approach has been important in the study of bromodomains are detailed below.

I-BET762 was amongst the first high affinity BET bromodomain ligands reported.^[22a, 32] It was discovered through phenotypic screening for compounds that upregulate apolipoprotein (ApoA1) expression, which is associated with protection against progression of atherosclerosis and anti-inflammatory effects.^[105] An initial hit, compound **49**, was identified but its cellular target or targets were unknown. Screening a panel of known drug targets did not identify a possible mode of action for **49**, so an affinity matrix based on the analogue **50** was generated. Using HepG2 cells, a chemoproteomic approach was taken to identify the cellular targets of these ligands, which resulted in the identification of BRD2-4. Subsequent biophysical assays confirmed the ligand binding *in vitro*.^[22b] This work underpinned the development of I-BET762 (**51**, Figure 11), which is currently in clinical trials.^[106] It is notable that these initial BET bromodomain ligands were identified using phenotypic screening. It is now a widely-recognized characteristic that BET bromodomain ligands display a strong phenotype, while ligands for other bromodomains, which have been developed using a structure-based design approach, have typically displayed weaker phenotypes. Removing the BET activity has been a key challenge in the development of probes for other families of bromodomains, especially CREBBP, so that their activity is not contaminated by residual weak inhibition of BET bromodomain function.

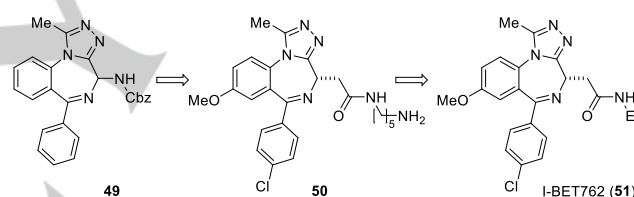


Figure 11. The BET bromodomain ligand I-BET762 (**51**) developed by scientists at GSK from an initial triazolobenzodiazepine (TBDZ) hit (**49**).^[22b, 106b] Compound **50** was attached to agarose beads to generate the affinity matrix for proteomic studies.^[22b]

5.2. Photo-crosslinking probes for bromodomains

More recent affinity-based bromodomain probes have employed covalent linking to their cellular targets coupled with the inclusion of a “click” tag. The advantage of covalent cross linking is that interactions across a spectrum of affinities can be investigated. A potential disadvantage is that very weak binders will be pulled down. The click tag allows the attachment of fluorophores to enable cellular imaging, and biotin to allow pull-down of the bound proteins. An additional advantage of the click tags is that they tend to be smaller, and hence cause less structural disruption, compared to the permanent inclusion of a fluorophore or biotin. This means that the protein-ligand interactions should be minimally affected, and cellular permeability will also be retained.

The first examples of small molecule photo-crosslinking probes for bromodomains were reported by Li *et al.*^[107] The TBDZ-based compounds **52** and **53** (Figure 12A) feature a bifunctional linker with both an alkyl diazine and a cyclopropene moiety. Upon UV-

REVIEW

irradiation ($\lambda = 350$ nm) the diaziridine generates a carbene intermediate, which covalently crosslinks to the targeted protein. The cyclopropene unit is used as a chemically tractable, and relatively small, tag suitable for copper-free biorthogonal click coupling to a tetrazine-labeled fluorophore (Figure 12B). The utility of this approach has been demonstrated by covalently labelling BRD4 in HepG2 cells for *in situ* imaging. Due to their applicability in native biological systems, Cu-free approaches including cyclopropene-tetrazine ligations are superior to concepts that are based on Cu(I)-catalysed alkyne-azide cycloadditions (CuAAC),^[108] e.g. **54** (Figure 12A). Use of the cyclopropene-tetrazine pair has the advantage that the tetrazine quenches the fluorescence of the unbound tetrazine-containing fluorophore reporter. After ligation to the cyclopropene, the resulting pyridazine does not quench the fluorescence. Consequently, the fluorescence of the attached fluorophore is “turned on”, allowing a reduction of background fluorescence. Coupling of a range of functionalized tetrazines, including biotin-linked tetrazines, allowed photo-affinity pull-down experiments to be conducted. Interestingly, **53** was observed to bind to 161 proteins, and **54** bound 117 proteins in HepG2 cells, highlighting the point that these probes pull down weakly interacting proteins. Of these proteins, 48 were bound by both probes and 14 of these were localized in the nucleus. Of these proteins, nine were identified as being likely off-targets of (+)-JQ1, which is structurally-related to the probes.

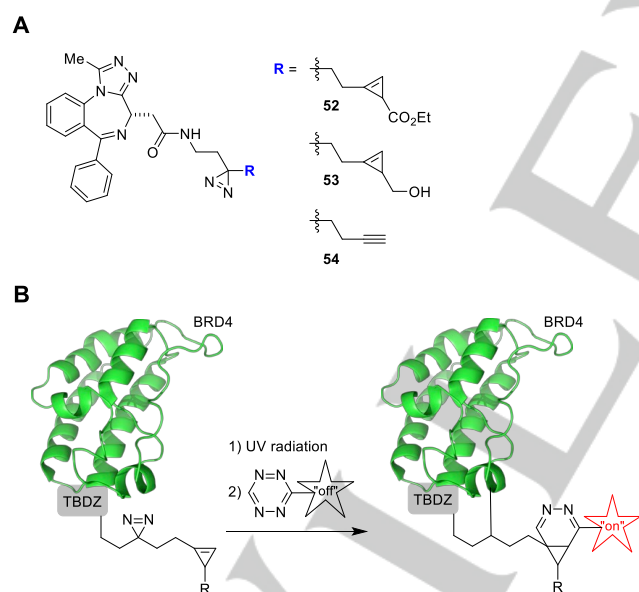


Figure 12. A) Photo-cross-linking probes **52–54** for bromodomains designed by Li *et al.*^[107] B) UV irradiation induces a covalent crosslink of the bi-functionalized triazolobenzodiazepine (TBDZ) to BRD4. In a second step the cyclopropene moiety is conjugated with the tetrazine-linked fluorescence reporter by Cu-free cyclopropene-tetrazine ligation.

Hett *et al.* developed a photoaffinity probe for the CREBBP and BET bromodomains (Figure 13) based on the CREBBP ligand SGC-CBP30 (**55**, $IC_{50} = 236$ nM for BRD4(1) and 274 nM for

CREBBP).^[82, 109] The key deviation from SGC-CBP30 is the exchange of the 3,5-dimethylisoxazole KAc mimic for a tropolone methyl ester, which was shown to be a photoreactive KAc mimic (Figure 13). After binding of the probe to the protein, irradiation at 365 nm gives rise to a covalent bond between the probe and protein. Colchicine and related natural products that feature tropolone moieties were also found to be micromolar ligands for BRD4 and can be used for photo-labelling approaches as well. A two-step labelling mechanism is proposed, in which the photoactivation of the tropolone gives rise to a reactive intermediate, which then undergoes reaction with the protein. However, the structure of the intermediate is not known. The authors propose ligation occurs by [2+2] cycloaddition, which has been reported for other tropolones.^[110] The propargyl group of **57** enables conjugation with an azide-containing reporter molecule or affinity tag (e.g. biotin) *via* CuAAC. The formation of a covalent protein-ligand adducts, with BRD4 and CREBBP, was observed using mass spectrometry. An attractive feature of these photoaffinity probes is that the photoreactive group is embedded within the ligand, offering unbiased, minimum assumption, assessment of the cellular target engagement and selectivity of the compound in question.

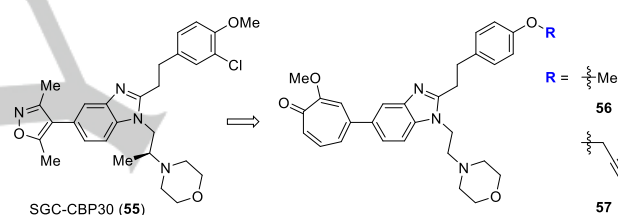


Figure 13. Development of the BET and CREBBP bromodomain photoaffinity probes **56–57** from SGC-CBP30 (**55**) reported by Hett *et al.*^[109]

5.3. Covalent binding of small molecule probes to bromodomains

Reaction of a ligand with its partner protein to form a covalent bond leads to compounds with prolonged residence times. Consequently, covalent binders display high protein affinity while having relatively low molecular mass, leading to beneficial pharmacokinetic properties.^[111] By reacting with a nucleophilic protein residue that is unique or rare across a protein family, covalent inhibition can also lead to increased selectivity against closely related proteins.^[112]

Inspired by activity-based profiling,^[113] and the emergence of useful covalent kinase inhibitors, Daguer *et al.*^[89b] sought to identify covalent ligands for bromodomains. They initially focused on the P300/CREBBP-associated factor (PCAF) bromodomain, and performed an affinity screen using a library of PNA-encoded small-molecule fragments combinatorially displayed on a DNA microarray. From this screen two compounds, **58** and **59** (Figure 14) were identified as ligands for the PCAF bromodomain. Both compounds feature an ethacrynic acid core, which undergoes conjugate addition with cysteine residues to form a covalent bond to the bromodomain binding partner. Biotinylated analogues of **58** and **59** were found to enrich BRD4, amongst other bromodomains, from MV4;11 leukemia cell lysates. Both probes were, however,

found to react with a number of off-target proteins, including those which do not contain bromodomains, meaning they would require further development to be suitable for future *in vivo* applications.^[89b]

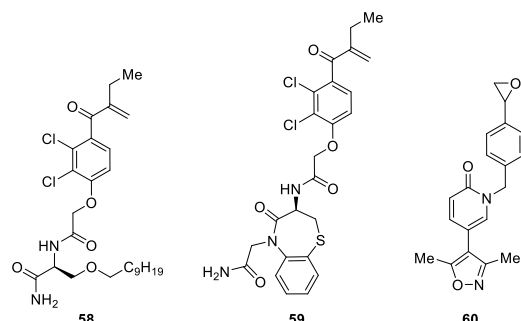


Figure 14. Covalent crosslinking probes that undergo conjugate addition with cysteine residues (**58–59**) or alkylate a methionine residue with their epoxide warhead (**60**).^[89b, 114]

Recent work by Kharenko *et al.* has led to the development of a new class of covalent BRD4(1) ligands, exemplified by **60** (Figure 14). An X-ray crystal structure confirmed that the compounds form a covalent bond with Met149 which is located close to the WPF shelf of BRD4(1). As this residue is not present in other bromodomain KAc binding pockets the compounds show good selectivity. In MV4;11 cells these covalent inhibitors exerted more durable anti-proliferative effects and decreased mRNA expression of several BET-dependent genes compared to reversible BET bromodomain inhibition.^[114] This is the first example of Met residue being targeted for covalent inhibition, and the Met-epoxide combination offers the possibility that further selective covalent ligands for other proteins can be developed by exploiting this pairing.

5.4. Small molecule-induced protein degradation applied to bromodomain-containing proteins

Proteolysis-targeting chimeras (PROTACs) are bifunctional molecules that comprise a ligand for an E3 ubiquitin ligase connected by a linker to a ligand for the target protein. They function by binding to both proteins, bringing them into close proximity. The E3 ligase associates with an E2 ligase, which polyubiquitinates the target protein, marking it for degradation by the proteasome.^[115] Currently, ligands for only four of over 600 E3 ligases, cereblon, cIAP, MDM2 and VHL, have been harnessed in for use in PROTACs. Most commonly employed are thalidomide and analogues leading to recruitment of cereblon, or ligands for the von Hippel-Lindau protein (VHL) leading to its recruitment. This approach, which has gained much traction recently, has a number of key differences to standard inhibition of protein function by small molecules, which has implications for basic research and potentially clinical applications. PROTACs induce degradation of the whole protein, making this approach more similar to knock-down or knock-out studies, rather than

occupancy-based inhibition. This is particularly important in the context of multidomain proteins, where the function of all domains is removed. In all cases, the scaffolding role of the protein is also removed. One advantage resulting from whole protein degradation is that “undruggable” protein domains can be degraded by targeting another domain in the same protein. Another key difference is that protein degradation can be catalytic, meaning that one PROTAC molecule can induce the degradation of multiple copies of the target protein. This is of particular importance in the context of PPI inhibition. Small molecules that inhibit the function of a receptor or an enzyme can also be thought of as catalytic, in that they inhibit the start of a cascade that might amplify a signal across a cell membrane (in the case of a receptor) or produce many products (in the case of an enzyme). Inhibitors of PPIs, including bromodomain ligands, are stoichiometric in the sense that one ligand prevents only one interaction between two proteins. Therefore, the amplification effect potentially enabled by a PROTAC approach will be particularly significant when it is applied to stoichiometric inhibitors, as opposed to catalytic inhibitors. As a consequence there is less need to maintain high *in vivo* concentrations of the compound to ensure sufficient efficacy, which potentially reduces the risk of off-target side effect.^[116]

5.4.1. Chemically induced degradation of BET bromodomains

The groups of Crews, Ciulli, and Bradner have employed known BET bromodomain ligands coupled to degradation-inducing entities to bring about selective intracellular elimination of BET proteins.^[117] These PROTACs all feature (+)-JQ1 or its close analogue OTX015 as the BET bromodomain-binding moiety, but differ in their linker region and the E3 ubiquitin ligase recruited (Figure 15).

The Crews group developed ARV-825 (**61**, Figure 15A),^[117b] which comprises OTX015, a small-molecule BRD4 ligand currently in phase I trials for selected advanced solid tumors^[118] and pomalidomide, an approved immunomodulatory drug (IMiD) known to act through binding to cereblon.^[119] These two portions are connected by a flexible polyethylene glycol linker; the high conformational flexibility of which increases the chance of the PROTAC binding to BRD4 and cereblon simultaneously, and additionally increases the water solubility of the chimera. ARV-825 (**61**) induces BRD4 degradation in Burkitt's lymphoma (BL) cells with a DC₅₀ value of < 1 nM (DC₅₀ is the concentration at which 50% degradation of the target protein occurs).^[117b] Treatment of BL cells with **61** caused significant reduction in the cellular levels of oncoprotein c-MYC and downstream cell proliferation. Notably, this effect was more pronounced upon **61** treatment than with either OTX015 or (+)-JQ1 alone, whose efficacy on c-MYC suppression is limited by inducing significant BRD4 accumulation. It was demonstrated that PROTAC treatment resulted in prolonged suppression of c-MYC. However, since OTX015 is not selective for BRD4, **61** also causes degradation of BRD2 and BRD3. In a similar approach Ciulli and

REVIEW

co-workers described the development of MZ1-3 (**62-64**, Figure 15B), which are based on (+)-JQ1.^[117a]

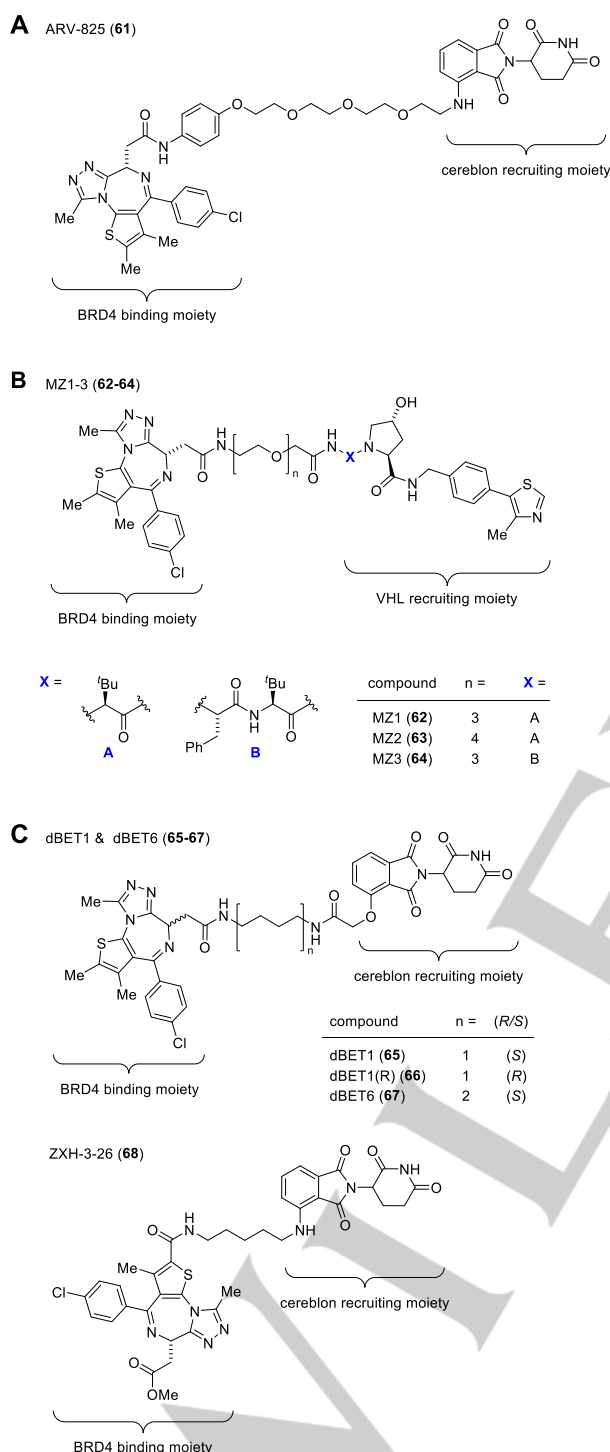


Figure 15. PROTACs (**61-68**) designed to target and subsequently induce degradation of the BET bromodomains.^[51b, 117, 120]

Compound **62** (Figure 15) features VHL-1, a small molecule developed by the Ciulli group that binds to the E3 ubiquitin ligase von Hippel-Lindau protein (VHL).^[121] In HeLa cells, **62** removed

more than 90% of all BET proteins at compound concentrations down to 1 μ M. The observation that compounds **62-64** showed preferential degradation of BRD4 over BRD2 and BRD3 indicated that the PROTACs concept could be an approach to gain selectivity for a certain bromodomain, even when starting from an unselective ligand (*vide infra*). Recently, Gadd *et al.* provided the structural basis of PROTAC cooperative recognition for selective protein degradation by solving the crystal structure of the ternary complex with MZ1 (**62**), BRD4(2), and VHL.^[122]

A further example of a BRD4-targeting PROTAC, dBET1 (**65**, Figure 15C), was characterized with a DC_{50} value of 430 nM, but did not show selectivity among the BET bromodomains. Compound **65** features the (+)-JQ1 scaffold as the BRD4-binding moiety. The E3 ubiquitin ligase cereblon-recruiting moiety is based on thalidomide,^[123] and is structurally similar to pomalidomide in ARV-825 (**61**). The efficacy with which **65** triggers BRD4 degradation was demonstrated in a number of human cancer cell lines. Studies in a murine xenograft model of human MV4;11 AML cells showed that **65** treatment slows tumor progression, and leads to reduced tumor size compared to vehicle control. Importantly, **65** was shown to be more beneficial than (+)-JQ1 treatment alone in a murine model of aggressive disseminated leukemia (mCherry⁺ MV4;11), demonstrating the benefit of BRD4 degradation over BRD4 inhibition *in vivo*.^[117c] In a follow up study, mechanistic characterization of the optimized analogue dBET6 (**67**), which features increased cellular activity with BET degradation evident in the sub-nanomolar range, led to the unexpected identification of BET bromodomains as master regulators of global transcription elongation. Unlike the selective effect of bromodomain inhibition on transcription, chemically-induced BET degradation provoked a collapse of global elongation that phenocopies CDK9 inhibition.^[51b] Guided by multiple X-ray crystal structures of further dBET analogues, co-crystallized in ternary complex with cereblon and BRD4(1), together with comprehensive biochemical, cellular, and computational characterization, Nowak *et al.* showed that the interaction between the E3 ligase and the substrate protein is plastic and can adapt distinct conformations depending on linker length and position. This finding guided the design of the BRD4-selective degrader ZXH-3-26 (**68**) that can discriminate between homologous BET bromodomains.^[120] The fact that pharmacological selectivity can be achieved through careful linker design inducing PPIs distal from the immediate binding site of the small molecule affords new opportunities for the development of target-specific degrader molecules.

Taken together, these publications highlight the advantages that can be achieved by applying BET-targeted PROTAC concepts compared to the occupancy-driven inhibition by compounds such as (+)-JQ1 or OTX015. They include improved efficacy in cell-based and animal models, improved BRD4 druggability by circumventing BRD4 accumulation upon pharmacological inhibition, and improved BRD4 subtype selectivity.

5.4.2. Chemically induced degradation of non-BET bromodomains

The PROTAC approach has also been applied to degradation of the non-BET bromodomain containing proteins, BRD9^[124] and TRIM24.^[44] Degradation of the multidomain bromodomain-containing transcriptional regulator TRIM24 using dTRIM24 (**69**, Figure 16) revealed that the RING domain, but not the bromodomain, of TRIM24 is responsible for the functional TRIM24 dependency of the leukemia cell lines MOLM-13 and MV4:11.^[44] This study is another example of the manner in which combination of probe molecules and PROTACs for the same target can reveal details of the target's biological function. dBRD9 (**70**) is a selective chemical degrader of BRD9. Its potent activity in cellular models of human AML was confirmed to be on target using proteomic studies.^[124] Most recently, Bassi *et al.* reported GSK699 (**71**), the first degrader of the multidomain bromodomain-containing transcriptional regulators PCAF and GCN5, which both containing an acetyltransferase domain and a bromodomain. While inhibition of the PCAF/GCN5 bromodomains was insufficient to recapitulate the diminished inflammatory response of PCAF deficient immune cells, degradation of PCAF/GCN5 potently modulates the expression of multiple inflammatory mediators in LPS-stimulated macrophages and dendritic cells.^[125] These results emphasize the utility of PROTACs in modulating the function of multi-domain proteins.

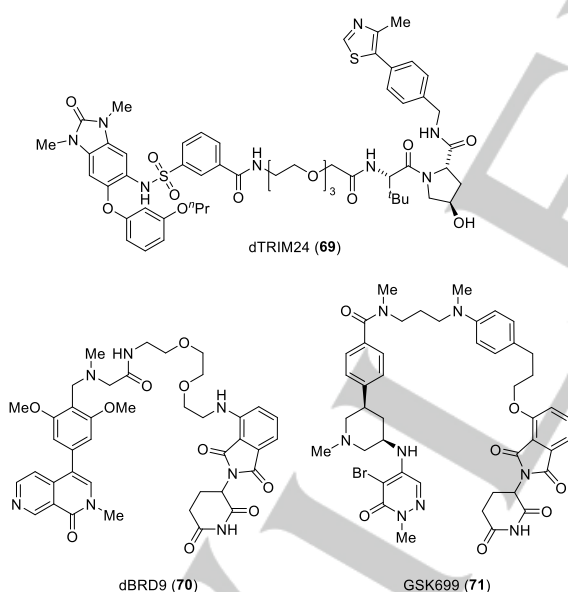


Figure 16. PROTACs (**69–71**) designed to target and subsequently induce degradation of the non-BET bromodomains TRIM24, BRD9, and PCAF/GCN5.^[44, 124–125]

5.4.3. Employing dTAGs to chemically induce bromodomain degradation

The dTAG system reported by Nabets *et al.* combines the principles of PROTACs, CRISPR Cas-9 with a bump-and-hole approach. To enable immediate and target-specific protein degradation the authors biochemically fused the protein FKBP12^{F36V} to the protein of interest, in this case BRD4. This was achieved by transgenic expression or CRISPR Cas-9 mediated locus-specific knock-in. A PROTAC was engineered comprising thalidomide and AP1867, a ligand that binds specifically to FKBP12^{F36V} variant but not to wild-type FKBP12. This bifunctional ligand specifically degraded BRD4-FKBP12^{F36V} fusion protein and not the other BET family bromodomains. Using this BRD4-FKBP12^{F36V} fusion targeted dTAG, in comparison with a pan-BET (+)-JQ1-based PROTAC (dBET6, **67**), the authors observed an unexpectedly higher antiproliferative effect of the pan-BET bromodomain degradation over the selective BRD4-FKBP12^{F36V} fusion-targeted degradation.^[126] This generally applicable strategy to study the immediate consequence of protein loss will have a major impact on target validation in drug discovery. It is especially applicable to proteins that are not suitable for a 'classical' PROTAC approach, e.g. due to the absence of ligands.

5.5. Bivalent probes for tandem bromodomains

The BET bromodomain-containing proteins all possess two bromodomains that are located proximal to each other.^[127] Given that there is relatively high homology between the first and second bromodomains of the BET proteins, and that most ligands for these proteins bind both domains with similar affinity, there is the opportunity to develop multivalent ligands. In contrast to PROTACs, the molecules discussed below are bivalent ligands of two domains located in the same protein. Multivalent interactions between a ligand and its target protein can enhance the affinity by more than 1,000-fold compared to the individual interactions, a phenomenon known as the avidity effect,^[128] consequently, multivalent inhibitors can also have prolonged residence times.^[129] The first bivalent bromodomain probes that were reported engage both bromodomains of BRD4 simultaneously.^[45, 130] More recently, a bivalent ligand for the non-BET bromodomain Transcription Initiation Factor TFIID subunit 1 (TAF1) has been reported.^[131]

Starting with the observation that compounds originally identified as androgen receptor (AR) down regulators show affinity for BRD4, Bradbury *et al.* developed the bivalent BRD4 inhibitor AZD5153 (**72**, Figure 17). The bivalent binding mode resulted in enhanced *in vitro* affinity ($pK_i = 8.3$), which directly translated into *c-Myc* modulation and tumor growth inhibition in a MV4:11 xenograft mouse model at low doses (10 mg/kg). This affinity, coupled with an excellent pharmacokinetic profile, led to **72** being selected as a clinical candidate for treatment of hematologic malignancies.^[130a, 132] By replacing the piperazinone moiety of **72** with a second triazolopyridazine Waring *et al.* developed the pseudosymmetric and bivalent BRD4 inhibitor biBET (**73**), with further increased affinity for BRD4, displaying a

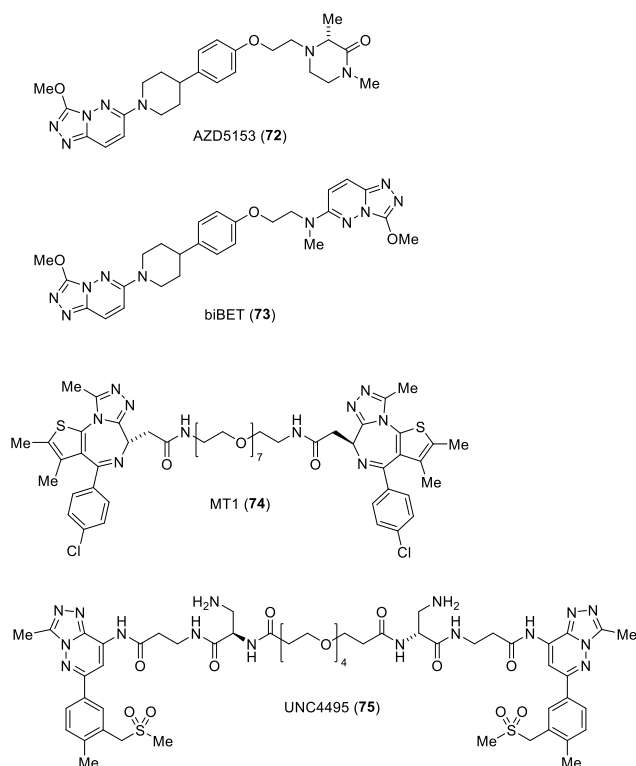


Figure 17. Bivalent ligands (**72–75**) for tandem bromodomains.^[45, 130–131]

pK_d value of 11. However, due to its unoptimized pharmacokinetic profile the authors suggest that **73** would be more valuable as a chemical probe than as a clinical candidate.^[130b] Further pseudosymmetric and bivalent BRD4 inhibitors were developed by joining two TBZs with linkers of different lengths. Among a series of synthesized compounds with different linker lengths and attachment points MT1 (**74**) was identified as the compound with the most promising pharmacodynamics and pharmacokinetic properties. Compound **74** showed a 400-fold increase in activity in AML cell lines (MV4;11) compared to the monovalent parent compound (+)-JQ1. Additionally, **74** significantly delayed leukemia progression in mice, compared to (+)-JQ1.^[45] Even though, all bivalent BRD4 ligand presented here show a significantly enhanced affinity, none of them shows a particular selectivity for BRD4 over the other members of the BET family. Nevertheless, these data provide a strong rationale for the further development of multivalent bromodomain inhibitors. Bivalent TAF1 ligands based on the promiscuous bromodomain ligand bromosporine have recently been reported by Suh *et al.*^[131, 133] The bivalent ligand UNC4495 (**75**) showed a >100-fold increase in affinity compared to its monovalent precursor. However, starting from the pan-bromodomain ligand bromosporine, the TAF1 selectivity of these bivalent ligands over other tandem bromodomains is unclear, as selectivity studies have not been performed yet.

6. Summary and outlook

The application of a wide range of techniques, spanning many disciplines has led to the emergence of bromodomains as an exciting and promising target class for therapeutic intervention. The application of key techniques in chemistry, chemical biology, and biochemistry aided the discovery and development of selective, high affinity small-molecule ligands with drug-like properties, for several bromodomains. For the bromodomain and extra terminal domain (BET) family, many ligands have been disclosed, and several BET bromodomain ligands are currently under investigation in clinical trials for the treatment of cancer. Potent and selective inhibitors for non-BET bromodomains have been also been reported: these novel tools will be important for a deeper understanding of the biological and pharmacological relevance of non-BET bromodomains. Given the major efforts and rapid progress in this research area, the development of further probes and novel drug candidates can be anticipated in the future. This work will provide a deeper understanding of the biology of bromodomains and open new avenues for the treatment of various diseases, perhaps beyond the oncology arena. It will be interesting to see if chemical biology concepts such as small molecule-induced protein degradation *via* PROTACs, co- or multivalent ligands, will contribute to the future clinical applications of bromodomain ligands. It will also be intriguing to see if some of the approaches established for bromodomains can be applied to the recently discovered, structurally diverse, KAc and crotonyl-lysine binding domains (YEATS).^[134]

Acknowledgements

M.S. is supported by the Deutsche Forschungsgemeinschaft (SCHI 1408/1-1). M. M., D. M. H. A., A. E. R. C., and J. J. A. G. K. are grateful to the EPSRC Centre for Doctoral Training in Synthesis for Biology and Medicine (EP/L015838/1) for studentships, generously supported by AstraZeneca, Diamond Light Source, Defence Science and Technology Laboratory, Evotec, GlaxoSmithKline, Janssen, Novartis, Pfizer, Syngenta, Takeda, UCB and Vertex. J. J. A. G. K. is also supported by a Clarendon Scholarship. A. R. S. thanks Pfizer Neusentis and the EPSRC for studentships support. S.J.C. thanks the MRC (MR/N009460/1) and St Hugh's College, Oxford, for funding.

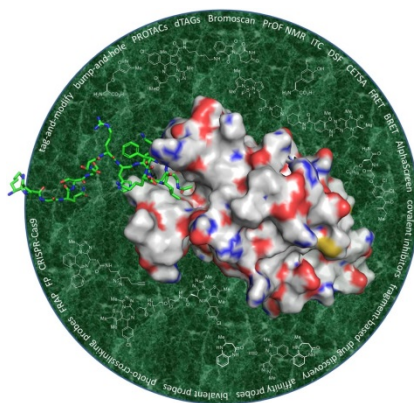
Keywords: Bromodomains • Epigenetics • Inhibitors • Protein-protein-interactions • PROTACs

- [1] C. H. Waddington, *Endeavour* **1942**, *1*, 18–20.
- [2] S. L. Berger, T. Kouzarides, R. Shiekhhattar, A. Shilatifard, *Genes Dev.* **2009**, *23*, 781–783.
- [3] M. J. Booth, E. A. Raiber, S. Balasubramanian, *Chem. Rev.* **2015**, *115*, 2240–2254.
- [4] K. D. Meyer, S. R. Jaffrey, *Nat. Rev. Mol. Cell Biol.* **2014**, *15*, 313–326.
- [5] a) C. H. Arrowsmith, C. Bountra, P. V. Fish, K. Lee, M. Schapira, *Nat. Rev. Drug Discov.* **2012**, *11*, 384–400; b) M. M. Muller, T. W. Muir, *Chem. Rev.* **2015**, *115*, 2296–2349; c) Z. Su, J. M. Denu, *ACS Chem. Biol.* **2016**, *11*, 564–574.
- [6] a) B. D. Strahl, C. D. Allis, *Nature* **2000**, *403*, 41–45; b) T. Jenuwein, C. D. Allis, *Science* **2001**, *293*, 1074–1080; c) B. M. Turner, *Cell* **2002**, *111*, 285–291; d) K. E. Gardner, C. D. Allis, B. D. Strahl, *J. Mol. Biol.* **2011**, *409*, 36–46.

- [7] a) F. Winston, C. D. Allis, *Nat. Struct. Biol.* **1999**, *6*, 601-604; b) C. Dhalluin, J. E. Carlson, L. Zeng, C. He, A. K. Aggarwal, M. M. Zhou, *Nature* **1999**, *399*, 491-496; c) T. Kouzarides, *EMBO J.* **2000**, *19*, 1176-1179; d) L. Zeng, M. M. Zhou, *FEBS Lett.* **2002**, *513*, 124-128; e) P. Filippakopoulos, S. Knapp, *FEBS Lett.* **2012**, *586*, 2692-2704.
- [8] G. D. Gregory, C. R. Vakoc, T. Rozovskaia, X. Zheng, S. Patel, T. Nakamura, E. Canaan, G. A. Blobel, *Mol. Cell. Biol.* **2007**, *27*, 8466-8479.
- [9] X. J. Yang, V. V. Ogryzko, J. Nishikawa, B. H. Howard, Y. Nakatani, *Nature* **1996**, *382*, 319-324.
- [10] E. Cavellan, P. Asp, P. Percipalle, A. K. O. Farrants, *J. Biol. Chem.* **2006**, *281*, 16264-16271.
- [11] W. W. Tsai, et al., *Nature* **2010**, *468*, 927-932.
- [12] Y. T. Xue, J. C. Canman, C. S. Lee, Z. Q. Nie, D. F. Yang, G. T. Moreno, M. K. Young, E. D. Salmon, W. D. Wang, *Proc. Natl. Acad. Sci. U. S. A.* **2000**, *97*, 13015-13020.
- [13] K. N. Hariharan, et al., *Nat. Genet.* **2005**, *37*, 254-264.
- [14] a) V. Bres, S. M. Yoh, K. A. Jones, *Curr. Opin. Cell Biol.* **2008**, *20*, 334-340; b) S. Y. Wu, C. M. Chiang, *J. Biol. Chem.* **2007**, *282*, 13141-13145.
- [15] P. Filippakopoulos, et al., *Cell* **2012**, *149*, 214-231.
- [16] M. Brand, et al., *ACS Chem. Biol.* **2015**, *10*, 22-39.
- [17] D. Z. Huang, E. Rossini, S. Steiner, A. Cafisch, *Chemmedchem* **2014**, *9*, 573-579.
- [18] E. M. Flynn, O. W. Huang, F. Poy, M. Oppikofer, S. F. Bellon, Y. Tang, A. G. Cochran, *Structure* **2015**, *23*, 1801-1814.
- [19] a) B. S. Gerstenberger, et al., **2016**, *59*, 4800-4811; b) O. Fedorov, et al., *Sci. Adv.* **2015**, *1*, e1500723; c) C. L. Sutherell, et al., *J. Med. Chem.* **2016**, *59*, 5095-5101; d) V. Myrianthopoulos, et al., *J. Med. Chem.* **2016**, *59*, 8787-8803.
- [20] M. Aldeghi, G. A. Ross, M. J. Bodkin, J. W. Essex, S. Knapp, P. C. Biggin, *Commun. Chem.* **2018**, *1*, 19.
- [21] a) P. Filippakopoulos, S. Knapp, *Nat. Rev. Drug Discov.* **2014**, *13*, 337-356; b) S. Muller, P. Filippakopoulos, S. Knapp, *Expert Rev. Mol. Med.* **2011**, *13*, 1-21; c) R. K. Prinjha, J. Witherington, K. Lee, *Trends Pharmacol. Sci.* **2012**, *33*, 146-153; d) A. C. Belkina, G. V. Denis, *Nat. Rev. Cancer* **2012**, *12*, 465-477.
- [22] a) E. Nicodeme, et al., *Nature* **2010**, *468*, 1119-1123; b) C. W. Chung, et al., *J. Med. Chem.* **2011**, *54*, 3827-3838.
- [23] a) D. S. Hewings, T. P. Rooney, L. E. Jennings, D. A. Hay, C. J. Schofield, P. E. Brennan, S. Knapp, S. J. Conway, *J. Med. Chem.* **2012**, *55*, 9393-9413; b) L. E. Jennings, A. R. Measures, B. G. Wilson, S. J. Conway, *Future Med. Chem.* **2014**, *6*, 179-204; c) D. Gallenkamp, K. A. Gelato, B. Haendler, H. Weinmann, *ChemMedChem* **2014**, *9*, 438-464; d) F. A. Romero, A. M. Taylor, T. D. Crawford, V. Tsui, A. Cote, S. Magnuson, *J. Med. Chem.* **2016**, *59*, 1271-1298.
- [24] www.clinicaltrials.gov.
- [25] M. Schiedel, S. J. Conway, *Curr. Opin. Chem. Biol.* **2018**, *45*, 166-178.
- [26] D. J. Owen, P. Ornaghi, J. C. Yang, N. Lowe, P. R. Evans, P. Ballarín, D. Neuhaus, P. Filetici, A. A. Travers, *EMBO J.* **2000**, *19*, 6141-6149.
- [27] a) W. Q. Shen, C. Xu, W. Huang, J. H. Zhang, J. E. Carlson, X. M. Tu, J. H. Wu, Y. Y. Shi, *Biochemistry* **2007**, *46*, 2100-2110; b) T. Umehara, Y. Nakamura, M. K. Jang, K. Nakano, A. Tanaka, K. Ozato, B. Padmanabhan, S. Yokoyama, *J. Biol. Chem.* **2010**, *285*, 7610-7618.
- [28] Z. Wang, J. Song, T. A. Milne, G. G. Wang, H. Li, C. D. Allis, D. J. Patel, *Cell* **2010**, *141*, 1183-1194.
- [29] M. Philpott, et al., *Epigenet. Chromatin* **2014**, *7*, 14.
- [30] W. Zhang, J. R. Bone, D. G. Edmondson, B. M. Turner, S. Y. Roth, *EMBO J.* **1998**, *17*, 3155-3167.
- [31] a) M. Jung, et al., *J. Biol. Chem.* **2014**, *289*, 9304-9319; b) M. G. Baud, et al., *Science* **2014**, *346*, 638-641; c) J. Schulze, D. Moosmayer, J. Weiske, A. Fernandez-Montalvan, C. Herbst, M. Jung, B. Haendler, B. Bader, *J. Biomol. Screen.* **2015**, *20*, 180-189.
- [32] P. Filippakopoulos, et al., *Nature* **2010**, *468*, 1067-1073.
- [33] M. Philpott, et al., *Mol. Biosyst.* **2011**, *7*, 2899-2908.
- [34] F. M. Ferguson, D. M. Dias, J. P. Rodrigues, H. Wienk, R. Boelens, A. M. Bonvin, C. Abell, A. Ciulli, *Biochemistry* **2014**, *53*, 6706-6716.
- [35] a) M. Benkirane, R. F. Chun, H. Xiao, V. V. Ogryzko, B. H. Howard, Y. Nakatani, K. T. Jeang, *J. Biol. Chem.* **1998**, *273*, 24898-24905; b) S. Mujtaba, Y. He, L. Zeng, A. Farooq, J. E. Carlson, M. Ott, E. Verdini, M. M. Zhou, *Mol. Cell* **2002**, *9*, 575-586.
- [36] V. Bres, H. Tagami, J. M. Peloponese, E. Loret, K. T. Jeang, Y. Nakatani, S. Emiliani, M. Benkirane, R. E. Kiernan, *EMBO J.* **2002**, *21*, 6811-6819.
- [37] a) J. Morinier, et al., *Nature* **2009**, *461*, 664-668; b) T. Kanno, Y. Kanno, R. M. Siegel, M. K. Jang, M. J. Lenardo, K. Ozato, *Mol. Cell* **2004**, *13*, 33-43.
- [38] M. D. Olp, N. Zhu, B. C. Smith, *Biochemistry* **2017**, *56*, 5485-5495.
- [39] J. D. Sander, J. K. Joung, *Nat. Biotechnol.* **2014**, *32*, 347-355.
- [40] C. Fellmann, B. G. Gowen, P. C. Lin, J. A. Doudna, J. E. Corn, *Nat. Rev. Drug Discov.* **2017**, *16*, 89-100.
- [41] U. Unniyampurath, R. Pilankatta, M. N. Krishnan, *Int. J. Mol. Sci.* **2016**, *17*, 291.
- [42] J. Shi, E. Wang, J. P. Milazzo, Z. Wang, J. B. Kinney, C. R. Vakoc, *Nat. Biotechnol.* **2015**, *33*, 661-667.
- [43] P. K. Mazur, et al., *Nat. Med.* **2015**, *21*, 1163-1171.
- [44] L. N. Gchijian, et al., *Nat. Chem. Biol.* **2018**, *14*, 405-412.
- [45] M. Tanaka, J. M. Roberts, H. S. Seo, A. Souza, J. Paulk, T. G. Scott, S. L. DeAngelo, S. Dhe-Paganon, J. E. Bradner, *Nat. Chem. Biol.* **2016**, *12*, 1089-1096.
- [46] a) E. F. Ullman, et al., *Proc. Natl. Acad. Sci. U. S. A.* **1994**, *91*, 5426-5430; b) A. Yasgar, A. Jadhav, A. Simeonov, N. P. Coussens, *Methods Mol. Biol.* **2016**, *1439*, 77-98.
- [47] a) D. S. Hewings, et al., *J. Med. Chem.* **2011**, *54*, 6761-6770; b) S. Picaud, et al., *Cancer Res.* **2013**, *73*, 3336-3346; c) A. E. Fernandez-Montalvan, et al., *ACS Chem. Biol.* **2017**, *12*, 2730-2736; d) V. S. Gehling, et al., *ACS Med. Chem. Lett.* **2013**, *4*, 835-840.
- [48] a) J. Wu, et al., *MedChemComm* **2014**, *5*, 1871-1878; b) M. R. McKeown, et al., *J. Med. Chem.* **2014**, *57*, 9019-9027; c) P. G. Clark, D. J. Dixon, P. E. Brennan, *Drug Discovery Today: Technol.* **2016**, *19*, 73-80.
- [49] M. A. Dawson, et al., *Nature* **2011**, *478*, 529-533.
- [50] a) N. Wang, F. D. Li, H. Y. Bao, J. Li, J. H. Wu, K. Ruan, *ChemBioChem* **2016**, *17*, 1456-1463; b) F. M. Ferguson, et al., *J. Med. Chem.* **2013**, *56*, 10183-10187; c) A. M. Ayoub, et al., *J. Med. Chem.* **2017**, *60*, 4805-4817.
- [51] a) L. W. Koblan, et al., *ChemMedChem* **2016**, *11*, 2575-2581; b) G. E. Winter, et al., *Mol. Cell* **2017**, *67*, 5-18; c) M. M. Savitski, et al., *Science* **2014**, *346*, 1255784.
- [52] M. B. Robers, et al., *Nat. Commun.* **2015**, *6*, 10091.
- [53] a) L. J. Martin, et al., *J. Med. Chem.* **2016**, *59*, 4462-4475; b) T. Machleidt, et al., *ACS Chem. Biol.* **2015**, *10*, 1797-1804; c) E. H. Demont, et al., *ACS Med. Chem. Lett.* **2014**, *5*, 1190-1195; d) M. Moustakim, et al., *Angew. Chem. Int. Ed.* **2017**, *56*, 827-831; *Angew. Chem.* **2017**, *129*, 845-849.
- [54] a) B. Raux, et al., *J. Med. Chem.* **2016**, *59*, 1634-1641; b) R. P. Law, et al., *J. Med. Chem.* **2018**, *61*, 4317-4334.
- [55] A. Bishop, et al., *Annu. Rev. Biophys. Biomol. Struct.* **2000**, *29*, 577-606.
- [56] A. C. Runcie, et al., *Chem. Sci.* **2018**, *9*, 2452-2468.
- [57] K. Lang, J. W. Chin, *Chem. Rev.* **2014**, *114*, 4764-4806.
- [58] J. M. Chalker, G. J. Bernardes, B. G. Davis, *Acc. Chem. Res.* **2011**, *44*, 730-741.
- [59] S. B. Shuker, P. J. Hajduk, R. P. Meadows, S. W. Fesik, *Science* **1996**, *274*, 1531-1534.
- [60] L. Zeng, J. Li, M. Muller, S. Yan, S. Mujtaba, C. Pan, Z. Wang, M. M. Zhou, *J. Am. Chem. Soc.* **2005**, *127*, 2376-2377.
- [61] a) Sachchidanand, L. Resnick-Silverman, S. Yan, S. Mutjaba, W. J. Liu, L. Zeng, J. J. Manfredi, M. M. Zhou, *Chem. Biol.* **2006**, *13*, 81-90; b) J. C. Borah, et al., *Chem. Biol.* **2011**, *18*, 531-541.
- [62] C. W. Chung, A. W. Dean, J. M. Woolven, P. Bamborough, *J. Med. Chem.* **2012**, *55*, 576-586.
- [63] B. J. Stockman, C. Dalvit, *Prog. Nucl. Magn. Reson. Spectrosc.* **2002**, *41*, 187-231.
- [64] a) W. C. Pomerantz, N. K. Wang, A. K. Lipinski, R. R. Wang, T. Cierpicki, A. K. Mapp, *ACS Chem. Biol.* **2012**, *7*, 1345-1350; b) C. T. Gee, E. J. Koleski, W. C. K. Pomerantz, *Angew. Chem. Int. Ed.* **2015**, *54*, 3735-3739; *Angew. Chem.* **2015**, *127*, 3806-3810; c) E. N. Marsh, Y. Suzuki, *ACS Chem. Biol.* **2014**, *9*, 1242-1250; d) X. Ge, et al., *J. Med. Chem.* **2014**, *57*, 6419-6427.
- [65] a) M. A. Danielson, J. J. Falke, *Annu. Rev. Biophys. Biomol. Struct.* **1996**, *25*, 163-195; b) J. L. Kiteviski-LeBlanc, R. S. Prosser, *Prog. Nucl. Magn. Reson. Spectrosc.* **2012**, *62*, 1-33.
- [66] A. Bondi, *J. Phys. Chem.* **1964**, *68*, 441-451.
- [67] A. A. Bogan, K. S. Thorn, *J. Mol. Biol.* **1998**, *280*, 1-9.
- [68] J. Gavenonis, B. A. Sheneman, T. R. Siegert, M. R. Eshelman, J. A. Kritzer, *Nat. Chem. Biol.* **2014**, *10*, 716-722.
- [69] B. N. Bullock, A. L. Jochim, P. S. Arora, *J. Am. Chem. Soc.* **2011**, *133*, 14220-14223.
- [70] A. M. Watkins, P. S. Arora, *ACS Chem. Biol.* **2014**, *9*, 1747-1754.
- [71] K. E. Arntson, W. C. Pomerantz, *J. Med. Chem.* **2016**, *59*, 5158-5171.
- [72] C. Frieden, S. D. Hoeltzli, J. G. Bann, *Methods Enzymol.* **2004**, *380*, 400-415.
- [73] a) L. Wang, A. Brock, B. Herberich, P. G. Schultz, *Science* **2001**, *292*, 498-500; b) K. V. Loscha, A. J. Herlt, R. Qi, T. Huber, K. Ozawa, G. Otting, *Angew. Chem. Int. Ed.* **2012**, *51*, 2243-2246; *Angew. Chem.* **2012**, *124*, 2286-2289.
- [74] P. A. Luchette, R. S. Prosser, C. R. Sanders, *J. Am. Chem. Soc.* **2002**, *124*, 1778-1781.
- [75] a) N. K. Mishra, A. K. Urlick, S. W. Ember, E. Schonbrunn, W. C. Pomerantz, *ACS Chem. Biol.* **2014**, *9*, 2755-2760; b) A. K. Urlick, et al., *ACS Chem. Biol.* **2015**, *10*, 2246-2256.
- [76] C. T. Gee, K. E. Arntson, A. K. Urlick, N. K. Mishra, L. M. L. Hawk, A. J. Wisniewski, W. C. K. Pomerantz, *Nat. Protoc.* **2016**, *11*, 1414-1427.
- [77] a) J. T. Guo, J. Y. Wang, J. S. Lee, P. G. Schultz, *Angew. Chem. Int. Ed.* **2008**, *47*, 6399-6401; *Angew. Chem.* **2008**, *120*, 6499-6501; b) F. Li, A. Allahverdi, R. Yang, G. B. Lua, X. Zhang, Y. Cao, N. Korolev, L.

- Nordenskiöld, C. F. Liu, *Angew. Chem. Int. Ed.* **2011**, *50*, 9611-9614; *Angew. Chem.* **2011**, *123*, 9785-9788; c) N. Jamonnak, B. M. Hirsch, Y. Pang, W. P. Zheng, *Bioorg. Chem.* **2010**, *38*, 17-25; d) B. M. Hirsch, W. P. Zheng, *Mol. Biosyst.* **2011**, *7*, 16-28; e) F. Zhang, Q. Zhou, G. Yang, L. An, F. Li, J. Wang, *Chem. Commun.* **2018**, *54*, 3879-3882; f) B. C. R. Dancy, et al., *J. Am. Chem. Soc.* **2012**, *134*, 5138-5148; g) A. Dose, et al., *Angew. Chem. Int. Ed.* **2016**, *55*, 1192-1195; *Angew. Chem.* **2016**, *128*, 1208-1211; h) D. G. Fatkins, A. D. Monnot, W. Zheng, *Bioorg. Med. Chem. Lett.* **2006**, *16*, 3651-3656.
- [78] S. Mujtaba, et al., *Mol. Cell* **2004**, *13*, 251-263.
- [79] N. Jamonnak, D. G. Fatkins, L. Wei, W. Zheng, *Org. Biomol. Chem.* **2007**, *5*, 892-896.
- [80] R. Huang, et al., *J. Am. Chem. Soc.* **2010**, *132*, 9986-9987.
- [81] L. E. Jennings, et al., *Bioorg. Med. Chem.* **2018**, *26*, 2937-2957.
- [82] D. A. Hay, et al., *J. Am. Chem. Soc.* **2014**, *136*, 9308-9319.
- [83] A. R. Sekirnik Nee Measures, D. S. Hewings, N. H. Theodoulou, L. Jursins, K. R. Lewendon, L. E. Jennings, T. P. Rooney, T. D. Heightman, S. J. Conway, *Angew. Chem. Int. Ed.* **2016**, *55*, 8353-8357; *Angew. Chem.* **2016**, *128*, 8493-8497.
- [84] C. W. Murray, D. C. Rees, *Nat. Chem.* **2009**, *1*, 187-192.
- [85] a) C. W. Murray, D. A. Erlanson, A. L. Hopkins, G. M. Keseru, P. D. Leeson, D. C. Rees, C. H. Reynolds, N. J. Richmond, **2014**, *5*, 616-618; b) J. S. Scott, M. J. Waring, *Bioorg. Med. Chem.* **2018**, *26*, 3006-3015.
- [86] A. L. Hopkins, G. M. Keseru, P. D. Leeson, D. C. Rees, C. H. Reynolds, *Nat. Rev. Drug Discov.* **2014**, *13*, 105-121.
- [87] D. A. Erlanson, R. S. McDowell, T. O'Brien, *J. Med. Chem.* **2004**, *47*, 3463-3482.
- [88] T. W. Johnson, R. A. Gallego, M. P. Edwards, *J. Med. Chem.* **2018**, *61*, 6401-6420.
- [89] a) P. Bamborough, H. Diallo, J. D. Goodacre, L. Gordon, A. Lewis, J. T. Seal, D. M. Wilson, M. D. Woodrow, C. W. Chung, *J. Med. Chem.* **2012**, *55*, 587-596; b) J. P. Daguer, C. Zambaldo, D. Abegg, S. Barluenga, C. Tallant, S. Muller, A. Adibekian, N. Winssinger, *Angew. Chem. Int. Ed.* **2015**, *54*, 6057-6061; *Angew. Chem.* **2015**, *127*, 6155-6159; c) P. V. Fish, et al., *J. Med. Chem.* **2012**, *55*, 9831-9837; d) H. T. Zhao, L. Gartenmann, J. Dong, D. Spiliotopoulos, A. Cafilisch, *Bioorg. Med. Chem. Lett.* **2014**, *24*, 2493-2496; e) L. Hoffer, et al., *J. Med. Chem.* **2018**, *61*, 5719-5732.
- [90] P. Bamborough, C. W. Chung, *MedChemComm* **2015**, *6*, 1587-1604.
- [91] a) E. H. Demont, et al., *J. Med. Chem.* **2015**, *58*, 5649-5673; b) P. Bamborough, et al., *J. Med. Chem.* **2015**, *58*, 6151-6178; c) P. Bamborough, et al., *Angew. Chem. Int. Ed.* **2016**, *55*, 11382-11386; *Angew. Chem.* **2016**, *128*, 11554-11558; d) D. C. Miller, et al., *Org. Biomol. Chem.* **2018**, *16*, 1843-1850.
- [92] W. S. Palmer, et al., *J. Med. Chem.* **2016**, *59*, 1440-1454.
- [93] a) M. Xu, A. Unzue, J. Dong, D. Spiliotopoulos, C. Nevado, A. Cafilisch, *J. Med. Chem.* **2016**, *59*, 1340-1349; b) A. Unzue, M. Xu, J. Dong, L. Wiedmer, D. Spiliotopoulos, A. Cafilisch, C. Nevado, *J. Med. Chem.* **2016**, *59*, 1350-1356; c) A. M. Taylor, et al., *ACS Med. Chem. Lett.* **2016**, *7*, 531-536.
- [94] P. L. Chen, et al., *J. Med. Chem.* **2016**, *59*, 1410-1424.
- [95] O. B. Cox, et al., *Chem. Sci.* **2016**, *7*, 2322-2330.
- [96] N. H. Theodoulou, et al., *J. Med. Chem.* **2016**, *59*, 1425-1439.
- [97] P. G. K. Clark, et al., *Angew. Chem. Int. Ed.* **2015**, *54*, 6217-6221; *Angew. Chem.* **2015**, *127*, 6315-6319.
- [98] A. M. Taylor, et al., *ACS Med. Chem. Lett.* **2016**, *7*, 145-150.
- [99] C. K. Jaladanki, N. Taxak, R. A. Varikoti, P. V. Bharatam, *Chem. Res. Toxicol.* **2015**, *28*, 2364-2376.
- [100] P. P. Sharp, J.-M. Garnier, D. C. S. Huang, C. J. Burns, **2014**, *5*, 1834-1842.
- [101] B. K. Albrecht, et al., *J. Med. Chem.* **2016**, *59*, 1330-1339.
- [102] a) M. J. Harner, B. A. Chauder, J. Phan, S. W. Fesik, *J. Med. Chem.* **2014**, *57*, 9687-9692; b) A. Chaikuad, A. M. Petros, O. Fedorov, J. Xu, S. Knapp, *MedChemComm* **2014**, *5*, 1843-1848.
- [103] P. Bamborough, et al., *J. Med. Chem.* **2018**, *61*, 8321-8336.
- [104] S. X. Pfister, A. Ashworth, *Nat. Rev. Drug Discov.* **2017**, *16*, 241-263.
- [105] P. J. Barter, S. Nicholls, K. A. Rye, G. M. Anantharamaiah, M. Navab, A. M. Fogelman, *Circ. Res.* **2004**, *95*, 764-772.
- [106] a) E. Ferri, C. Petosa, C. E. McKenna, *Biochem. Pharmacol.* **2016**, *106*, 1-18; b) O. Mirguet, et al., *J. Med. Chem.* **2013**, *56*, 7501-7515.
- [107] Z. Li, D. Wang, L. Li, S. Pan, Z. Na, C. Y. Tan, S. Q. Yao, *J. Am. Chem. Soc.* **2014**, *136*, 9990-9998.
- [108] a) H. C. Kolb, K. B. Sharpless, *Drug Discovery Today* **2003**, *8*, 1128-1137; b) P. Y. Yang, K. Liu, M. H. Ngai, M. J. Lear, M. R. Wenk, S. Q. Yao, *J. Am. Chem. Soc.* **2010**, *132*, 656-666; c) H. Shi, C. J. Zhang, G. Y. Chen, S. Q. Yao, *J. Am. Chem. Soc.* **2012**, *134*, 3001-3014.
- [109] E. C. Hett, et al., *MedChemComm* **2015**, *6*, 1018-1023.
- [110] a) K. Tanaka, R. Nagahiro, Z. Urbanczyk-Lipkowska, *Org. Lett.* **2001**, *3*, 1567-1569; b) W. G. Dauben, K. Koch, O. L. Chapman, S. L. Smith, *J. Am. Chem. Soc.* **1963**, *85*, 2616-2621.
- [111] A. J. T. Smith, X. Y. Zhang, A. G. Leach, K. N. Houk, *J. Med. Chem.* **2009**, *52*, 225-233.
- [112] J. Singh, E. M. Dobrusin, D. W. Fry, T. Haske, A. Whitty, D. J. McNamara, *J. Med. Chem.* **1997**, *40*, 1130-1135.
- [113] D. K. Nomura, M. M. Dix, B. F. Cravatt, *Nat. Rev. Cancer* **2010**, *10*, 630-638.
- [114] O. A. Kharenko, et al., *J. Med. Chem.* **2018**, *61*, 8202-8211.
- [115] A. C. Lai, C. M. Crews, *Nat. Rev. Drug Discov.* **2017**, *16*, 101-114.
- [116] M. Toure, C. M. Crews, *Angew. Chem. Int. Ed.* **2016**, *55*, 1966-1973; *Angew. Chem.* **2016**, *128*, 2002-2010.
- [117] a) M. Zengerle, K. H. Chan, A. Ciulli, *ACS Chem. Biol.* **2015**, *10*, 1770-1777; b) J. Lu, et al., *Chem. Biol.* **2015**, *22*, 755-763; c) G. E. Winter, D. L. Buckley, J. Paulk, J. M. Roberts, A. Souza, S. Dhe-Paganon, J. E. Bradner, *Science* **2015**, *348*, 1376-1381.
- [118] a) M. Boi, et al., *Clin. Cancer Res.* **2015**, *21*, 1628-1638; b) A. Stathis, et al., *Cancer Discovery* **2016**, *6*, 492-500.
- [119] G. Lu, R. E. Middleton, H. Sun, M. Naniong, C. J. Ott, C. S. Mitsiades, K. K. Wong, J. E. Bradner, W. G. Kaelin, Jr., *Science* **2014**, *343*, 305-309.
- [120] R. P. Nowak, et al., *Nat. Chem. Biol.* **2018**, DOI 10.1038/s41589-41018-40055-y.
- [121] C. Galdeano, M. S. Gadd, P. Soares, S. Scaffidi, I. Van Molle, I. Bircsed, S. Hewitt, D. M. Dias, A. Ciulli, *J. Med. Chem.* **2014**, *57*, 8657-8663.
- [122] M. S. Gadd, A. Testa, X. Lucas, K.-H. Chan, W. Chen, D. J. Lamont, M. Zengerle, A. Ciulli, *Nat. Chem. Biol.* **2017**, *13*, 514-521.
- [123] T. Ito, H. Ando, T. Suzuki, T. Ogura, K. Hotta, Y. Imamura, Y. Yamaguchi, H. Handa, *Science* **2010**, *327*, 1345-1350.
- [124] D. Remillard, et al., *Angew. Chem. Int. Ed.* **2017**, *56*, 5738-5743; *Angew. Chem.* **2017**, *129*, 5832-5837.
- [125] Z. I. Bassi, et al., *ACS Chem. Biol.* **2018**, DOI 10.1021/acscchembio.1028b00705.
- [126] B. Nabet, et al., *Nat. Chem. Biol.* **2018**, *14*, 431-441.
- [127] M. K. Jang, K. Mochizuki, M. S. Zhou, H. S. Jeong, J. N. Brady, K. Ozato, *Mol. Cell* **2005**, *19*, 523-534.
- [128] M. Monsigny, R. Mayer, A. C. Roche, *Carbohydr. Lett.* **2000**, *4*, 35-52.
- [129] A. Bach, C. N. Chi, G. F. Pang, L. Olsen, A. S. Kristensen, P. Jemth, K. Stromgaard, *Angew. Chem. Int. Ed.* **2009**, *48*, 9685-9689; *Angew. Chem.* **2009**, *121*, 9865-9869.
- [130] a) R. H. Bradbury, et al., *J. Med. Chem.* **2016**, *59*, 7801-7817; b) M. J. Waring, et al., *Nat. Chem. Biol.* **2016**, *12*, 1097-1104.
- [131] J. L. Suh, et al., *Biochemistry* **2018**, *57*, 2140-2149.
- [132] G. W. Rhyasen, et al., *Mol. Cancer Ther.* **2016**, *15*, 2563-2574.
- [133] S. Picaud, et al., *Sci. Adv.* **2016**, *2*, e1600760.
- [134] a) F. H. Andrews, et al., *Nat. Chem. Biol.* **2016**, *12*, 396-398; b) Q. Zhang, L. Zeng, C. C. Zhao, Y. Ju, T. Konuma, M. M. Zhou, *Structure* **2016**, *24*, 1606-1612; c) Y. Y. Li, D. Zhao, Z. L. Chen, H. T. Li, *Transcription* **2017**, *8*, 9-14.

REVIEW



REVIEW

Text for Table of Contents